

INTERFIBER FRICTION AS RELATED TO FIBER DIAMETER

A THESIS

Presented to

The Faculty of the Graduate Division

by

Carl Raeford Cuthbertson, Jr.

In Partial Fulfillment

of the Requirements for the Degree

Master of Science

in the A. French Textile School

The Georgia Institute of Technology

May, 1970

GEORGIA INSTITUTE OF TECHNOLOGY LIBRARY

Regulations for the Use of Theses

Unpublished theses submitted for the Master's and Doctor's degrees and deposited in the Georgia Institute of Technology Library are open for inspection and consultation, but must be used with due regard for the rights of the authors. Passages may be copied only with permission of the authors, and proper credit must be given in subsequent written or published work. Extensive copying or publication of the thesis in whole or in part requires the consent of the Dean of the Graduate Division of the Georgia Institute of Technology.

This thesis by CARL RAEFORD CUTHBERTSON, Jr has been used by the following persons, whose signatures attest their acceptance of the above restrictions.

A library which borrows this thesis for use by its patrons is expected to secure the signature of each user.

NAME AND ADDRESS OF USER	BORROWING LIBRARY	DATE
--------------------------	-------------------	------

7777 7777

In presenting the dissertation as a partial fulfillment of the requirements for an advanced degree from the Georgia Institute of Technology, I agree that the Library of the Institute shall make it available for inspection and circulation in accordance with its regulations governing materials of this type. I agree that permission to copy from, or to publish from, this dissertation may be granted by the professor under whose direction it was written, or, in his absence, by the Dean of the Graduate Division when such copying or publication is solely for scholarly purposes and does not involve potential financial gain. It is understood that any copying from, or publication of, this dissertation which involves potential financial gain will not be allowed without written permission.

7/25/68

INTERFIBER FRICTION AS RELATED TO FIBER DIAMETER

Approved:

[Signature]

Date approved by Chairman: April 4, 1969

DEDICATED

To the memory of my thesis advisor

Mr. Richard B. Belser

ACKNOWLEDGMENTS

At the conclusion of this study, the author would like to express sincere appreciation and gratitude for the assistance shown him by the following persons:

Mr. Richard B. Belser, thesis advisor, for his invaluable aid and unselfish support which he so willingly offered.

Dr. James L. Taylor for providing a graduate assistantship and a T.E. Stribling fellowship to make possible this year of graduate study.

Mr. Billy R. Livesay for the use of his facilities and for his creative suggestions during the course of this investigation.

Mr. J. Conrad Meaders for his technical assistance and encouragement.

Dr. Gary W. Simmons for serving as a member of the reading committee.

Mr. J. W. McCarty for his assistance in obtaining the fibers necessary for this research and for serving as a member of the reading committee.

The author's wife, Mary Ellen, for her patience and understanding during this year of graduate study.

The author's parents, Mr. and Mrs. Carl R. Cuthbertson, for their assistance, encouragement and many kindnesses throughout the undergraduate and graduate years spent at the Georgia Institute of Technology.

TABLE OF CONTENTS

	Page
ACKNOWLEDGMENTS	iii
LIST OF TABLES	vi
LIST OF ILLUSTRATIONS	viii
SUMMARY	x
Chapter	
I. INTRODUCTION	1
Statement of the Problem	
Objective and Method of Attack	
II. LITERATURE SURVEY	4
III. INSTRUMENTATION, MATERIALS, AND PROCEDURE	17
Introduction	
Low Normal Force Fiber Friction Apparatus	
Modifications	
Materials	
Measuring Procedure	
IV. EXPERIMENTAL WORK	36
General	
Effects of Fiber Size and Delusterant Content	
Sources of Error	
V. DISCUSSION OF RESULTS	56
Effects of Fiber Diameter and Normal Force	
Effect of Delusterant	
Statistical Evaluation	
VI. CONCLUSION AND RECOMMENDATIONS	65
Conclusions	
Recommendations	

TABLE OF CONTENTS (Continued)

	Page
APPENDIX	68
BIBLIOGRAPHY.	88

LIST OF TABLES

Table	Page
1. Specifications of Nylon 66 Fibers Investigated	27
2. Data Displaying Effects of Size and Delusterant on Friction of Nylon 66 Fibers	43
3. Computation of Static Friction (μ_s) Using the Average Value of the Stick Displacements on the Friction Plot	53
4. Calculation of Scale Factor " α "	69
5. Calculation of Integrator Constant.	70
6. Coefficients of Friction for Fiber Pairs of 7 Denier Type 280 Nylon 66	71
7. Coefficients of Friction for Fiber Pairs of 10 Denier Type 280 Nylon 66	73
8. Coefficients of Friction for Fiber Pairs of 15 Denier Type 280 Nylon 66	75
9. Coefficients of Friction for Fiber Pairs of 20 Denier Type 280 Nylon 66	77
10. Coefficients of Friction for Fiber Pairs of 15 Denier Type 90 Nylon 66	79
11. Coefficients of Friction for Fiber Pairs of 15 Denier Type 680 Nylon 66	80
12. Representative Values of the Coefficients of Friction for Textile Fibers as Reported by Various Investigators	82
13. Analysis of Variance for the Effect of Fiber Diameter upon μ_s at 10 mg Normal Force	84
14. Analysis of Variance for the Effect of Fiber Diameter upon μ_k at 10 mg Normal Force	85

LIST OF TABLES (Continued)

Table		Page
15.	Analysis of Variance for the Effect of Fiber Diameter upon μ_s at 20 mg Normal Force	86
16.	Analysis of Variance for the Effect of Fiber Diameter upon μ_k at 20 mg Normal Force	87

LIST OF ILLUSTRATIONS

Figure		Page
1.	Deformation of Crossed Fibers under Load	8
2.	Logarithmic Plot of Pascoe and Tabor's Results.	11
3.	Essential Features of Pascoe and Tabor's Fiber Friction Apparatus.	12
4.	Results of Varying Normal Force on Static Friction as Found by Pascoe and Tabor.	14
5.	Calibration Data for Electrically-Operated Normal Force Applicator.	21
6.	Calibration Data for Electrically-Operated Frictional Force Applicator.	24
7.	Calibration Data for Friction Sensing Apparatus.	25
8.	Scanning Electron Micrograph of Surface of 7 Denier Type 280 Nylon 66 Fiber	28
9.	Scanning Electron Micrograph of Surface of 10 Denier Type 280 Nylon 66 Fiber	28
10.	Scanning Electron Micrograph of Surface of 15 Denier Type 280 Nylon 66 Fiber	29
11.	Scanning Electron Micrograph of Surface of 20 Denier Type 280 Nylon 66 Fiber	29
12.	Scanning Electron Micrograph of Surface of 15 Denier Type 90 Nylon 66 Fiber.	30
13.	Scanning Electron Micrograph of Surface of 15 Denier Type 680 Nylon 66 Fiber	30
14.	Scanning Electron Micrograph of Surface Features of 20 Denier Type 280 Nylon 66 (4250 x)	31

LIST OF ILLUSTRATIONS (Continued)

Figure		Page
15.	Typical Frictional Plot for Fiber Pair of 7 Denier Type 280 (Semi-Dull) Nylon 66 at 10 mg Normal Force.	34
16.	Typical Frictional Plot for Fiber Pair of 10 Denier Type 280 (Semi-Dull) Nylon 66 at 10 mg Normal Force.	38
17.	Typical Frictional Plot for Fiber Pair of 15 Denier Type 280 (Semi-Dull) Nylon 66 at 10 mg Normal Force.	39
18.	Typical Frictional Plot for Fiber Pair of 20 Denier Type 280 (Semi-Dull) Nylon 66 at 10 mg Normal Force.	40
19.	Typical Frictional Plot for Fiber Pair of 15 Denier Type 90 (Bright) Nylon 66 at 10 mg Normal Force	41
20.	Typical Frictional Plot for Fiber Pair of 15 Denier Type 680 (Dull) Nylon 66 at 10 mg Normal Force	42
21.	Variation of μ_s and μ_k with Fiber Denier for Semi-Dull Nylon 66 Fibers.	44
22.	Variation of μ_s and μ_k with Fiber Diameter for Semi- Dull Nylon 66 Fibers.	45
23.	Variation of μ_s/μ_k with Fiber Denier for Semi-Dull Nylon 66 Fibers.	46
24.	Variation of μ_s/μ_k with Fiber Diameter for Semi-Dull Nylon 66 Fibers.	47
25.	Variation of μ_s with Normal Force for Nylon 66 Fibers	48
26.	Variation of μ_k with Normal Force for Nylon 66 Fibers	49
27.	Variation of μ_s/μ_k with Normal Force for Nylon 66 Fibers	50
28.	Comparison of μ_s and μ_k Versus Load for 15 Denier Type 280 (Semi-Dull) Nylon 66 Fibers	51

SUMMARY

The static and kinetic coefficients of friction between Nylon 66 fibers of a selected series of diameters have been measured in order to ascertain the manner in which the friction varies with the fiber diameter. The effect on friction of changes in the delusterant content of the fibers was also examined.

Friction measurements of a series of Nylon 66 fibers, in a range of 7 to 20 denier and containing approximately 0.02, 0.3, and 2.0 per cents respectively of titanium dioxide (TiO_2) delusterant were made with a servo-controlled measuring instrument at normal forces of 10 and 20 mg. The instrument displayed the measurements as a graphically recorded plot of the stick-slip data from which the desired numerical data could be determined.

It was found that the static and kinetic coefficients of friction of Nylon 66 increase as the fiber diameter increases in accordance with the expression

$\mu_2 = \mu_1 + .005 (D_2 - D_1)$, where D is expressed in microns. If the diameter is expressed in denier instead of microns, the factor 0.005 becomes 0.0077 for nylon of density 1.30 gms/cm^3 .

The values of the static and kinetic coefficients of friction decreased with increasing normal force. The data agreed essentially with the form of the expression proposed by Pascoe and Tabor that $\mu = W^{-0.26} D^{0.52}$ where μ was derived from the average for all stick values obtained for a fiber traverse. However, the value obtained in this research, over a more restricted range and for a somewhat

different fiber, fit the expression $\mu_k = sk W^{-0.21} D^{0.59}$. The coefficient μ_k is essentially equivalent to the coefficient, μ , reported by Pascoe and Tabor.

μ_s (derived from the ten highest sticks) was found to follow the form:

$$\mu_s = sk W^{-0.25} D^{0.40}.$$

The effect of the delusterant was not clearly defined. In general, the dull fibers (2.0 per cent TiO_2) gave higher μ_s and μ_k values at 15 denier than did the semi-dull fibers (0.3 per cent TiO_2); the bright variety of Nylon 66 (0.02 per cent TiO_2), which was of trilobal cross section, gave a value of μ_k between those of the dull and semi-dull 15 denier fibers; its μ_s value was higher than those of the other 15 denier fibers.

The character of the frictional plots revealed that the fibers containing the least delusterant featured many short duration (low energy) stick-slip cycles. The semi-dull variety showed longer duration (higher energy) cycles and the dull fibers showed the longest duration cycles (highest energy) of the three types. Ploughing by delusterant particles on the fiber surface was indicated at the higher load levels.

CHAPTER I

INTRODUCTION

Statement of the Problem

A series of reports and theses, prepared at the Georgia Institute of Technology and discussed in Chapter II of this work, has presented an intensive investigation of the friction of natural and man-made fibers as related to textile processing. In the various research endeavors it became apparent that despite numerous previous investigations of fiber friction, only a few individuals had reported on fiber diameter as a factor in the measurement of fiber friction. The size factor had been largely ignored. Control of diameters using natural fibers is difficult and allows only a limited range of variation. Most natural fibers have superimposed upon them a shape effect which is related to the size variation effect. The only known investigation where fiber diameter was explicitly considered was one in which only a summation of the static coefficient peak amplitudes was measured. No instrument was available at the time for furnishing a completely recorded series of data for fiber stick-slip motions at low normal forces. The presence of a suitable instrument and a wealth of man-made fiber sizes manufactured by the fiber industry made available the necessary equipment and materials for proper measurements. The need and pertinence of such measurements to better understand interfiber frictional performance are apparent to those participating in research and new fiber development.

A concurrent problem which exists is the effect of added delusterants, such as titanium dioxide (TiO_2), on the frictional behavior of man-made fibers. Such delusterants are added to man-made fibers to minimize glossiness and transparency and to improve certain fiber handling characteristics. The particular pertinence of fiber delusterant to the problem of size is that procurement of textile fibers completely lacking delusterant is difficult. It is evident that delusterant content affects fiber shape and fiber smoothness. These in turn will affect a measurement of the effect of fiber size on interfiber friction. The effects are probably greater for a small fiber than for a larger one. Man-made fibers containing quantities of delusterants in the range 0.02 to about 3 per cent are commonly produced and used in the yarn manufacturing industry. The surface roughening effect is important because it affects the area of contiguous fiber contact and the time of contact between fibers in relative motion to each other. Cotton is a small size fiber with shape and roughness features superimposed upon it as a result of its natural growth pattern. Wool and hair fibers exhibit roughness features caused by unidirectional scales. Other natural fibers are usually rough. Hence, it is apparent that a delineation of the effect of fiber delusterant on interfiber friction for a series of different fiber sizes is a desirable investigation and a necessary one to understand the friction of rough fibers and of fibers of selected sizes in which delusterants may or may not be present.

Objective and Method of Attack

The primary purpose of this investigation was to measure the static and kinetic coefficients of friction between fibers of a selected series of diameters

and to develop a relation which describes the manner in which the friction varies with the fiber diameter. A secondary objective was to determine the effects contributed by the delusterant to the fiber friction measurements. Hence, the effect of the diameter of the fiber on fiber friction in the presence of known percentages of delusterant was evaluated.

A series of Nylon 66 fibers was procured in a range of 7 to 20 denier containing three percentages respectively of TiO_2 delusterant, approximately 0.03, 0.2, and 2.0 per cents. Friction measurements of each fiber series were made on an instrument capable of giving the measurements as a graphically recorded plot of the stick-slip data. These were made at normal force levels of 10 and 20 mg. Calculations of the kinetic coefficient of friction, μ_k , the static coefficient of friction, μ_s , and the ratio μ_s/μ_k were made and correlated according to the varied parameters. Characters of selected curves were studied and interpreted. The results obtained were analyzed and compared to the friction versus fiber size or roughness effects reported by earlier investigators using somewhat less versatile instrumentation.

CHAPTER II

LITERATURE SURVEY

When a substance is moved across the surface of a solid, there exists a force which resists this motion. This force is known as friction. In studying the nature of friction, da Vinci, Coulomb, and Amontons (1) contributed to the presently accepted laws of friction for a macroscopic body moving across a second from rest or at a uniform velocity.

The frictional behavior of solids, including the historical development of friction concepts and methods of measurement, has been examined extensively by Bowden and Tabor (2) and some of their associates. In addition, they discussed friction of polymer and fiber materials. Their work has led to a surface interaction theory of friction which involves adhesion and actual welding over microzones. According to Bowden et. al., the area of real contact, A , equals W/P , where W is the load and P is the yield pressure of the material. Under the intense pressure at microzones and the resulting yield and flow of the material, the junctions weld together. For sliding to occur these junctions must be broken by shearing. The force to shear the junction is the frictional force, F , and is given by $F = A_s$, where A is the total area of the welded portions and s is the shear strength of the material under study.

The relation between load and area of real contact under elastic deformation conditions depends on the geometry of the contacts and the elastic properties of the

materials. These were formulated by Hertz (3) in 1881.

Lincoln (4) observed that the friction between a nylon sphere and a nylon plane surface was $F = kW^{2/3}$ when measured in the range of 1 gram to 100 grams. This result agreed with Hertz's solution for the elastic deformation of a spherical surface.

Lodge and Howell (5) studied three different contact cases: a sphere on a plane surface, crossed cylinders, and a string around a cylinder. For a sphere on a plane surface they concluded that the area of contact was proportional to $W^{8/9}$ and $R^{2/9}$, where W is the load and R is the radius of the sphere.

Howell, Mieszkis, and Tabor (6) have further discussed the frictional behavior of unlubricated surfaces of long-chain polymeric materials in bulk and fiber form. McBride, (7) Bryant, (8) Gunther, (9) and Huff (10) reviewed the history of fiber friction measurements and described improved methods for measuring friction between contiguous fibers.

When two fibers are placed in contact, the contiguous zone consists of only one or a few asperities from each fiber. This area of contact assumes vital importance in the measurement of friction between the fibers. Howell (11) observed that the relation $F = kW^n$ is valid for fibers, and he proposed to replace Amonton's law ($F = kW$) with the expression $F = kW^n$. He found the exponent, n , to be between 0.80 and unity.

Howell also discussed the relation in terms of Bowden's cohesion theory of friction previously outlined. He showed, however, that the areas of contact are determined by the visco-elastic properties of the surfaces and thus the contact

areas become a function of time as well as load. Hence, the frictional force between fibers is dependent upon the real area of contact at a given time for viscoelastic material. Measurements were made for a known time after contact was established.

The fact that the precise value of the exponent, n , in Howell's expression depends upon the deformation properties of the polymer was demonstrated by Huntington (12). He stated that the coefficient of friction μ varies as W^{n-1} and, thus, decreases as the load increases.

Howell and Mazur (13) found that for crossed fibers, the relation $F = k W^n$ was valid in the load range 0.3 to 400 mg. The values of the constants n and k depend upon the material being investigated. Their findings are as follows:

<u>Material</u>	<u>n</u>	<u>k</u>
Cellulose Acetate	0.96	0.60
Viscose Rayon	0.91	0.49
Drawn Nylon	0.80	0.92
Undrawn Nylon	0.90	0.85

Since the frictional force is proportional to the load raised to a power less than unity, it is seen that a given increase in load results in a somewhat smaller increase in frictional force. The coefficient of friction ($\mu = F/W$) hence decreases with higher loads.

In the data of Gunther (9) and Huff (10), it was discerned that a size effect existed in measuring the friction between fibers. This development was discussed

at some length by Belser and Taylor (14). A study of the work of Bowden and Tabor (2) and Belser and Taylor (14) in search of greater details on the size effect disclosed the work of Pascoe and Tabor (15). These investigators studied the effect of the diameter of crossed fibers which make contact over a microzone (Figure 1). They found that the diameter, d , of the apparent circle of contact, when plotted versus the load, fits the expression $W = kd^{2.7}$, where k is a constant, over a wide load range.

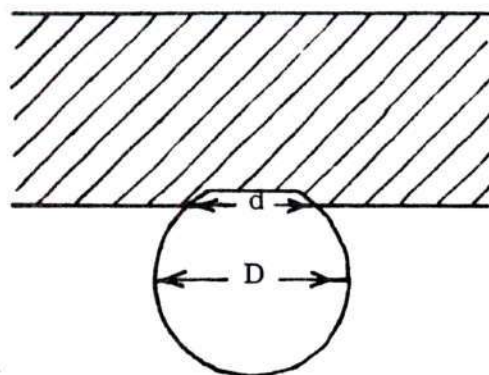
Pascoe and Tabor (16) also carried out experiments in which a series of indentations was made in bulk polymer (for a loading time of 15 seconds) with hard steel balls over a load range from 1 to 120 kg. The diameter d of the impression was measured, and the following relation found: $W = kd^n$, where n is between 2.5 and 2.7 for various polymers. Pascoe and Tabor applied dimensional analysis to the indentation process in the steps outlined below.

The ratio d/D determines the shape of the indentation where d is the chordal diameter of the indentation, and D the diameter of the hard sphere. Consequently, the mean pressure over the indentation $\left(\frac{4W}{\pi d^2}\right)$ is merely a function of d/D . If

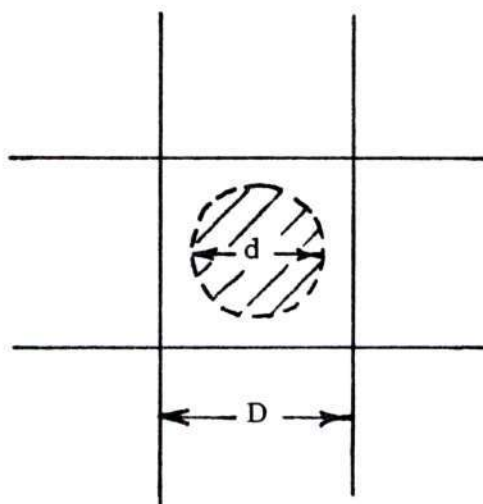
$$\left(\frac{4W}{\pi d^2}\right) = k_1 \left(\frac{d}{D}\right)^m, \quad (1)$$

incorporating $\frac{\pi k_1}{4}$ into a new constant k ,

$$W = k \frac{d^{m+2}}{D^m} = k \frac{d^n}{D^{n-2}} \quad (2)$$



(a) Section



(b) Plan

Figure 1. Deformation of Crossed Fibers under Load.

where $n = m + 2$ is the observed index. Then WD^{n-2} should be proportional to d^n . The projected area \bar{A} of the indentation is proportional to d^2 . Thus from equation (1)

$$\bar{A} = k \left(WD^{n-2} \right)^{2/n} = kW^{2/n} D^{(2n-4)/n}. \quad (3)$$

In order to extrapolate areal measurements to friction results, Pascoe and Tabor (16) made the following simplifying assumptions:

(1) The friction arises essentially from interfacial adhesion over the real area of contact A . This implies that F is directly proportional to the true contact area A , assuming that the specific shear strength of the interface is constant over the range of experiments performed.

(2) The true contact area A is to a first approximation the same as the indentation area \bar{A} . This is a crude approximation since the presence of asperities will always tend to make A less than \bar{A} .

(3) The true contact area during sliding is the same as the static area of contact.

(4) The deformation of crossed cylinders of a given radius is the same as the deformation of a flat surface by a sphere of the same radius. This implies that equation (3) applies equally to crossed fibers of diameter D .

It follows that the friction F should be proportional to \bar{A} . Since an increase in load also increases \bar{A} and F , one would reasonably expect the frictional coefficient μ to increase with higher loads. As was shown, however, an increased load results in a decrease in μ since the relative increase in F is less than the

increase in W . The frictional force is evidently affected more by changes in load ($F = kW^n$) than it is by changes in contact area. The coefficient of friction may be written

$$\mu = skW^{(2-n)/n} D^{(2n-4)/n}, \quad (4)$$

where s is the specific shear strength of the interface. This implies that if μ is known for any one value of W and D , the value of μ for any other value of W and D is determined solely in terms of the index n . The value of n was found to be 2.7 for undrawn nylon, giving the relation

$$\mu = skW^{-0.26} D^{0.52}.$$

Figure 2 shows that this relation fits the experimental results for undrawn nylon as reported by Pascoe and Tabor.

Pascoe and Tabor verified this expression with an instrument capable of measuring static friction between two fibers. The apparatus is shown in Figure 3. In this apparatus, a sliding cylindrical fiber is mounted at one end, while the second end rests against a second fiber mounted above it and at right angles to it. The upper fiber then serves as a cantilever with its vertical displacement providing the load. When the traversing fiber is moved, the upper fiber undergoes a horizontal displacement until the restoring force breaks the frictional contact, and the upper fiber slips back toward its zero position. Hence, a series of stick-slip motions of the upper fiber is registered and its displacement is a function of the frictional force applied to it by the traversing fiber. A load range of normal

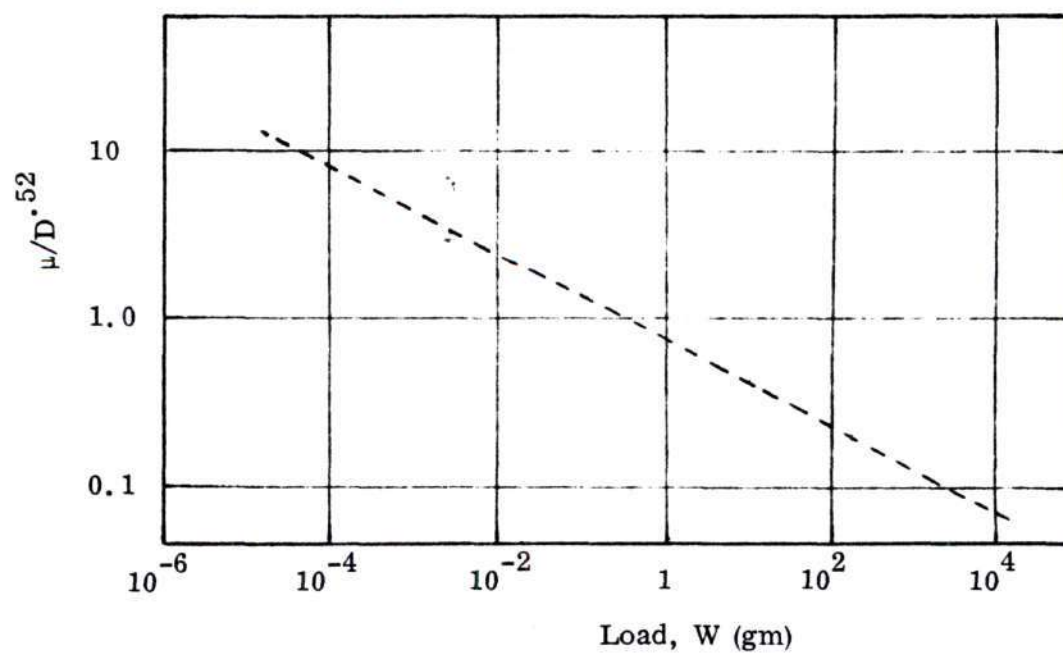


Figure 2. Logarithmic Plot of Pascoe and Tabor's Results: the Theoretical Straight Line of Slope -0.26 lies Close to the Experimental Points.

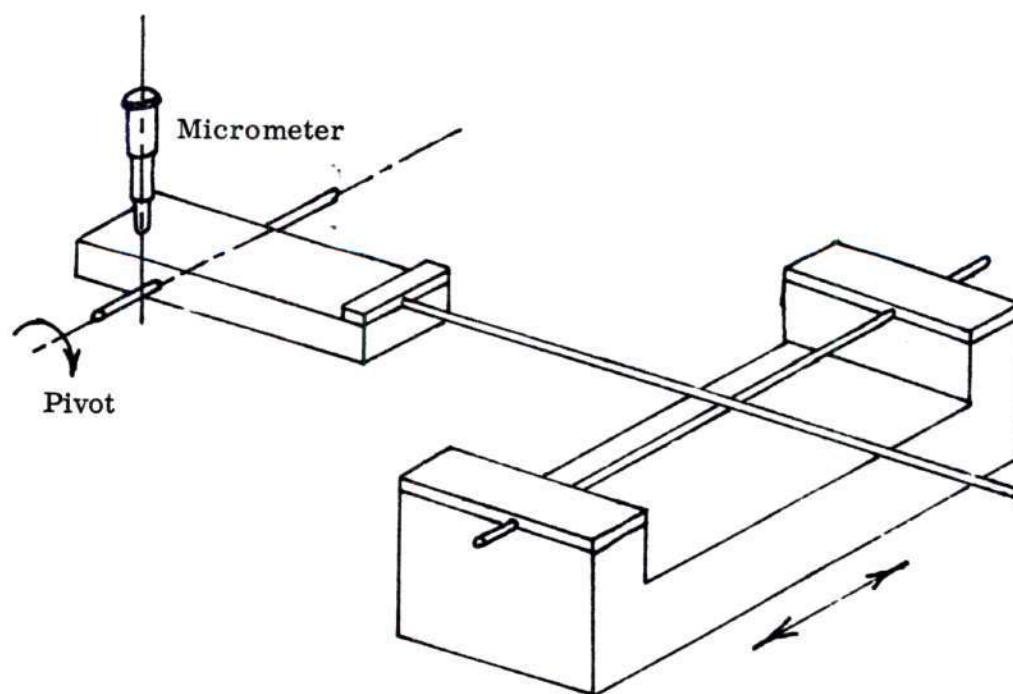


Figure 3. Essential Features of Pascoe and Tabor's Fiber Friction Apparatus.

forces of 0.001 mg to 1000 mg was examined by Pascoe and Tabor using a selection of fiber sizes and materials. Figure 4 depicts the data obtained by them for a series of fiber materials, using the instrument which they have described. For a nylon fiber 0.042 mm in diameter and a load of 10 mg, the coefficient of friction was found to be approximately 0.5. At lesser loads of about 1 mg it increased to 1.4. It must be emphasized that this instrument measured only each stick portion of the friction data, as there was no provision for determining a graphical data curve. However, subsequent studies (10, 14) confirmed that for smooth fibers the kinetic coefficient of friction was the value obtained from the method of summation of all stick values.

Pascoe and Tabor (16) showed that the frictional forces between pairs of crossed fibers of one diameter compared with those of a second diameter vary approximately as $D^{0.52}$ or essentially as $D^{1/2}$ if the load is maintained at a constant value. Since the denier of fibers of the same material varies as the diameter², friction between such fibers must vary essentially as denier^{1/4}.

The history of man-made fiber delusterants can be traced back to the 1930's. When rayon was first produced in the nineteenth century, its high luster was admired. Later, however, fashion changed and brightness and transparency became undesirable. Various ways of producing a dull (matt) or a semi-dull (pearl) appearance were devised (17). An early viscose rayon called Dulesco was dulled by the inclusion of tiny oil droplets dispersed in it, and cellulose acetate could be dulled by boiling it in water containing soap and phenol. But there were disadvantages attached to these methods, and for many years now the primary

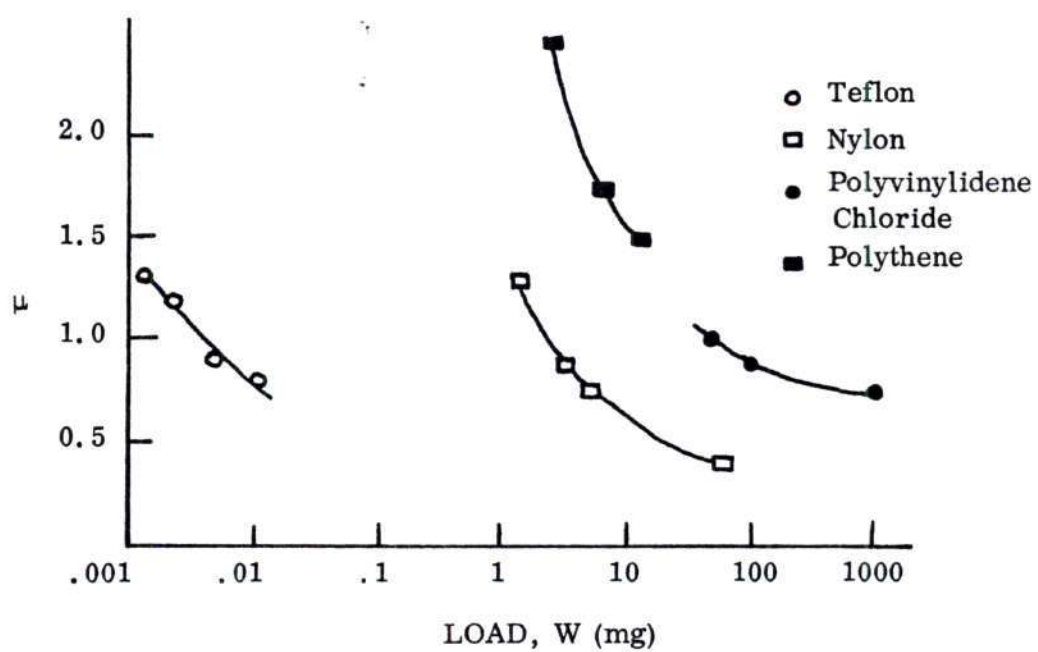


Figure 4. Results of Varying Normal Force on Static Friction as Found by Pascoe and Tabor.

delusterant has been dispersed particles of titanium dioxide. This compound is chemically inert and is unaffected by the wet processes to which yarns or fabrics are likely to be subjected. It has excellent covering power and is readily obtainable in particles of uniformly small size (0.05μ or smaller) which will not choke the spinneret. Investigators (17) have found that a matt fiber may, owing to the solid particles it contains near its surface, exert an abrasive action on parts of machinery in which it comes in contact, such as the heddles and reeds of a loom. Rapid wear of equipment may result.

A literature search of the effect of man-made fiber delusterants on fiber roughness and interfiber friction revealed that the majority of reported work in this area has been done at the Textile Research Institute, Princeton, New Jersey. Lyons (18) and Scheier and Lyons (19, 20) have recently reported methods of measuring fiber roughness and fiber friction with instruments developed at the Institute. Lyons (18) has shown that it is possible to obtain reproducible data related to the geometric roughness of the surface of a fiber by means of a probe connected to an electromagnetic transducer. Scheier and Lyons (19) examined two samples of Dacron containing 2.0 and 0.1 per cents, respectively, of TiO_2 delusterant. The former sample was found to have, on the average, from three to seven times as many asperities on the fiber surface as the other had, though the difference in average asperity heights between the two samples was less marked. These results indicate that the addition of more TiO_2 increased the number of asperities as expected. The constant heights indicate that the particle-size distributions of the TiO_2 were essentially the same in the two Dacron samples.

After passing the stylus of the instrument along the same portion of a specimen three times, Scheier and Lyons noted that some fiber asperities became more pronounced in the second and third passes over the fiber. It was speculated that in these cases a loosely held TiO_2 particle on the surface is removed in a test, producing a crevice (negative asperity) of greater absolute magnitude than the original asperity created by the particle. Scheier and Lyons (20) investigated specimens of 2-denier Dacron containing different amounts of titanium dioxide delusterant with a torsion wire suspension instrument. They found that the chart recordings for the bright sample (0.1 per cent TiO_2) showed many more short-duration stick-slip cycles than did those for dull (2.0 per cent TiO_2). The relation between these differences and the different delusterant contents of the two samples was not readily apparent. Scardino and Lyons (21, 22, 23) have applied the methods of Scheier and Lyons along with the ASTM static cohesion measuring method and a drafting analyzer to studies of surface and cohesive properties of Dacron polyester fiber specimens containing 0.1 and 2.0 per cents of titanium dioxide delusterant.

The findings of these investigators generally concur with the observations made by Belser and Taylor (14), which are that large smooth cylindrical fibers give large areas of contact, and that delusterant particles tend to roughen the fiber somewhat and lessen the area of contact between the polymers. Ploughing effects may also result. Finally, any element introduced to roughen the fibers, such as a delusterant, will reduce the number of contacts in a fiber bundle and will reduce the time of contact during an individual fiber traverse.

CHAPTER III

INSTRUMENTATION, MATERIALS, AND PROCEDURE

Introduction

Although abundant measurements of fiber friction have been made in the past by a number of investigators as noted in Chapter II, each method preceding the present one has usually had severe limitations to its use with respect to materials, normal force employed, fiber traverse rates, and the methods of data recording. In addition, experimental conditions have varied widely. The result has been that, in spite of the ample data, no clear understanding of fiber friction has been developed. The outstanding work of Bowden, Tabor, Pascoe, Howell, and many others has certainly laid the foundation from which further work may be profitably pursued. The apparatus employed by Pascoe and Tabor (16) was limited to the measurement of cylindrical fibers using slow traverse rates. Only very tedious and slow experiments could be conducted with this instrument. It appeared desirable to devise an instrument which would display a greater versatility with respect to each of these factors and, in particular, would permit rapid measurement, instrumental recording of data, and automatic integration to obtain the average kinetic frictional force in addition to the static frictional force measured by other methods. The genesis of the present instrument is described in the theses of McBride (7), Bryant (8), Gunther (9), and Huff (10).

An instrument for measuring fiber friction was designed and constructed at the Engineering Experiment Station, Georgia Institute of Technology, Atlanta, Georgia, which permitted the measuring of both the static and kinetic coefficients of friction between fiber pairs. The principal feature of this instrument was a servo-restored force-measuring sensor which allowed measurement of minute forces and furnished an electrical potential proportional to the force to an X-Y plotter. The first model of the apparatus was built by McBride under the supervision of Livesay (24) and is discussed in detail in McBride's thesis (7). The original instrument was limited in sensitivity and range of operation because of its bearings and the gravity method of setting normal force. A new instrument with improved sensitivity and data-taking ability was subsequently designed and constructed as discussed by Gunther (9).

Low Normal Force Fiber Friction Apparatus

The new apparatus for measuring interfiber friction utilized the same general principles on which the older instrument was built. However, the new instrument enabled frictional studies to be made at very low normal forces (< 2 mg) and design improvements allowed important parameters to be varied separately. The instrument employed a servo-mechanism designed by Livesay for measuring small torques on metal film specimens placed in a magnetic field (24). It made possible the translation of one fiber across another fiber at right angles to it and the simultaneous monitoring of the forces applied to the lower fiber. The lower fiber was mounted on the needle of a servo-controlled D'Arsonval galvanometer. As the upper fiber was traversed across the lower

fiber by the driving mechanism, the lower fiber and galvanometer needle were deflected. The deflection was detected by means of a mirror and light beam arrangement in which the light beam impinged upon a split photo-diode. A displacement of the beam caused an imbalance in the photo-diode. The servo-amplifier responded by sending a restoring current to the galvanometer coil to bring the beam and needle to the zero position. Simultaneously the current amplitude was monitored as a function of time or fiber translation with an X-Y recorder. The ordinate displacement of the pen was proportional to the frictional force between the fiber pairs and the displacement along the abscissa to the displacement of the traversing fiber from its starting position. The static and kinetic coefficients of friction for a given fiber pair were calculated from the data plot.

The improved instrument had incorporated into it an electro-magnetic system to apply the normal force between the fiber pair. A meter movement was attached to a milling vise such that the rotational axis of the meter was positioned in a horizontal plane. Connected to the coil of the meter movement was a small fiber-holding arm. A rough counterbalance was established by means of a small length of tubing on the opposite side of the coil, while fine balancing was obtained with the meter's normal zero adjustment mechanism. When a current was introduced into the coil, a force was produced at the end of the arm where the fiber was mounted. This force was directly proportional to the current supplied to the coil.

The force-current relation was determined by placing small known weights

on the mounted fiber and reversing the current by means of a switch. The current-normal force calibration data followed a linear relation over the desired range. Figure 5 displays typical calibration data. Electrical damping was used to minimize the tendency for the horizontal arm to bounce at low normal forces.

The instrument featured a variable speed motor which drove the loading device and the attached upper fiber at selected velocities. The velocity of fiber traverse ranged from .002 to .220 mm/sec. The motor was reversible by means of a simple switch and allowed rapid reversal of the traverse direction if desired.

Two types of fiber mounts were used. The lower fiber mount, applied to the servo-controlled galvanometer needle, consisted of a "U" shaped piece of beryllium copper. The upper fiber mount, applied to the arm of the low normal force instrument, was a "U" shaped piece of cupro-nickel tubing.

Gunther (9) improved the data-taking capability of the instrument by incorporating an integrator into the system. The $\int_{T_1}^{T_2} i dt$ which is proportional to the servo-signal during the traverse of one fiber across a second was measured. A value in volts proportional to the area defined by the frictional plot was obtained. The potential output signal from the servo was fed to the integrator at the same time that it was being fed to the X-Y recorder.

To insure adequate sensitivity to variations in the frictional force as a result of changes in the area of contact between the upper and lower fibers, Huff (10) refined the instrument further. He arranged both lateral and horizontal adjustment capabilities for positioning the dual photo-diode with respect to the light beam. An adjustable mount for the light source was also built. These changes

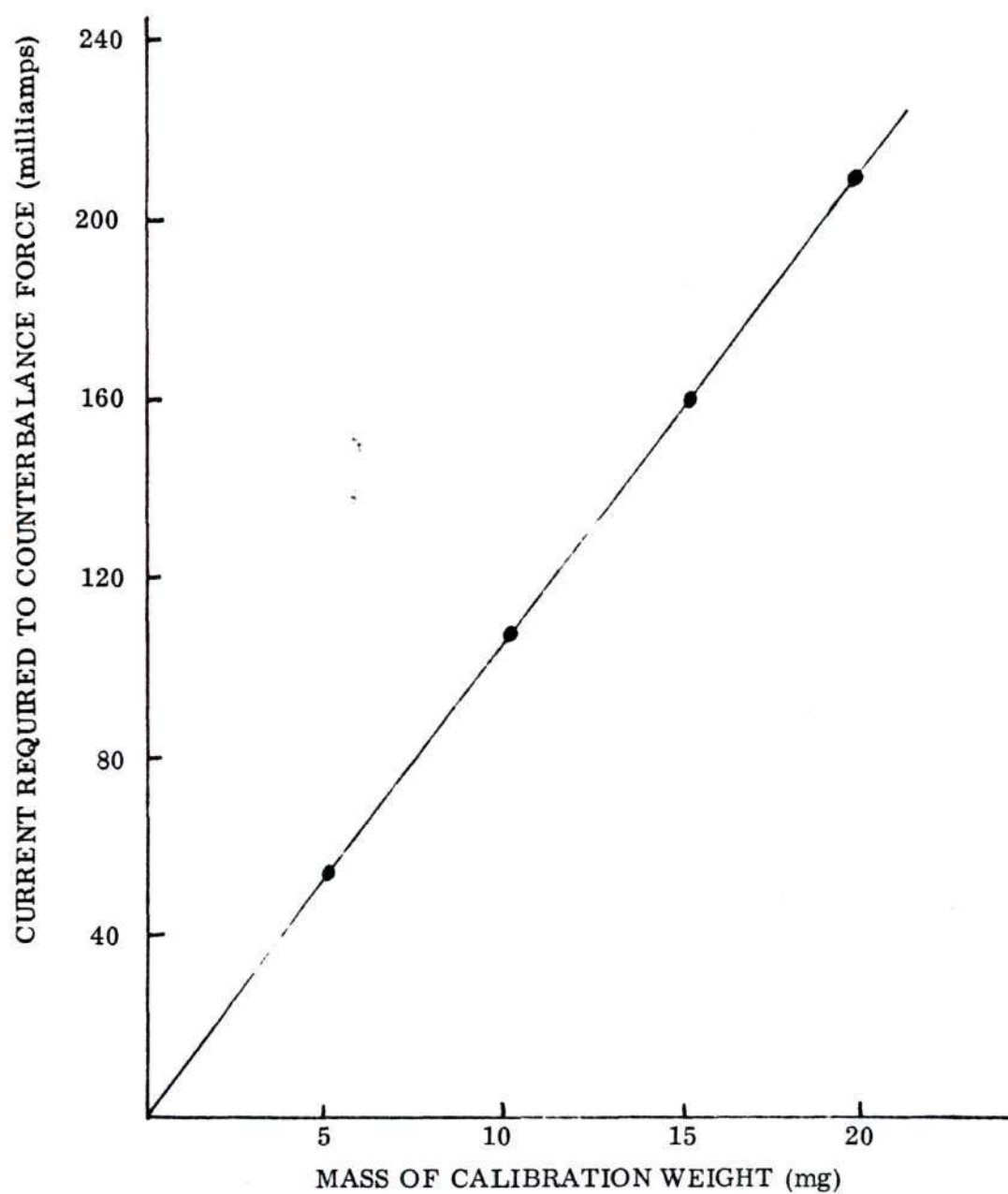


Figure 5. Calibration Data for Electrically-Operated Normal Force Applicator.

allowed one to maintain a correct image of the source on the dual photo-diode. Huff's final modification was a new and simpler method for calibrating the galvanometer sensor apparatus. The galvanometer deflection force constants on both the newer instrument and the original apparatus had been calibrated in the first series of measurements by turning the galvanometer and its associated sensor system on one side and hanging small known weights at a selected location on the needle. The current necessary to return the needle to its zero position was then recorded. At the same time, a potential proportional to the current was fed to the ordinate deflection of an X-Y recorder. A calibration constant in mg/volt was thus obtained. Huff improved on this practice by mounting a second electric meter movement on a plastic stand with the needle of the movement free to exert a force against an adjacent object. The arm from this meter movement rested against the arm of the frictional force sensor in its zero position. Calibration of the friction instrument and X-Y recorder could be made by passage of selected levels of electric current through the coil of this second meter movement. Forces representative of the force exerted against the sensing fiber of the friction measuring apparatus during its operation were applied by this electrical method. This applicator for a simulated frictional force was calibrated similarly to the normal force applicator. It was placed on one side and small known weights were hung successively on the arm at a selected point. The wires carrying current from the normal force control switch to the meter movement, which forms the normal force applicator, were disconnected from their terminals on the coil and were connected to the terminals provided on the back of the simulated frictional

force applicator-calibrator. The current reaching the calibrator was thus controlled by the same rheostat that regulated the normal force. The current was reversed with a three terminal switch, and the current required to bring the calibrator arm with a weight attached to a horizontal position was registered by a milliammeter. The horizontal position was determined by visual observation. Settings were repeatable within very small error limits. A linear relation between force and current resulted as shown in Figure 6. The linear relationship between force and current remained constant for the horizontal force calibrator in subsequent measurements up to a load of 25 mg. For proper calibration it was important that the arm contact the lower fiber at precisely the same lever arm distance of both the arm and the fiber support arm during each calibration. In turn, the point had to be the same at which the graduated weights were hung during the calibration step. After construction and calibration of the applicator, the frictional force sensing apparatus could be calibrated by placing the horizontal force applicator in position, using the same electrical connections as described in its calibration, and reversing the current as before. The applicator arm exerted a force against and slightly displaced the lower fiber of the friction sensing apparatus. Current to counterbalance the force was supplied and the force was recorded by the X-Y plotter in the form of an ordinate displacement of the recorder pen. A milliammeter registered the current required to produce the displacement. A current versus ordinate pen displacement relationship of linear form was observed and typical data are exhibited in Figure 7.

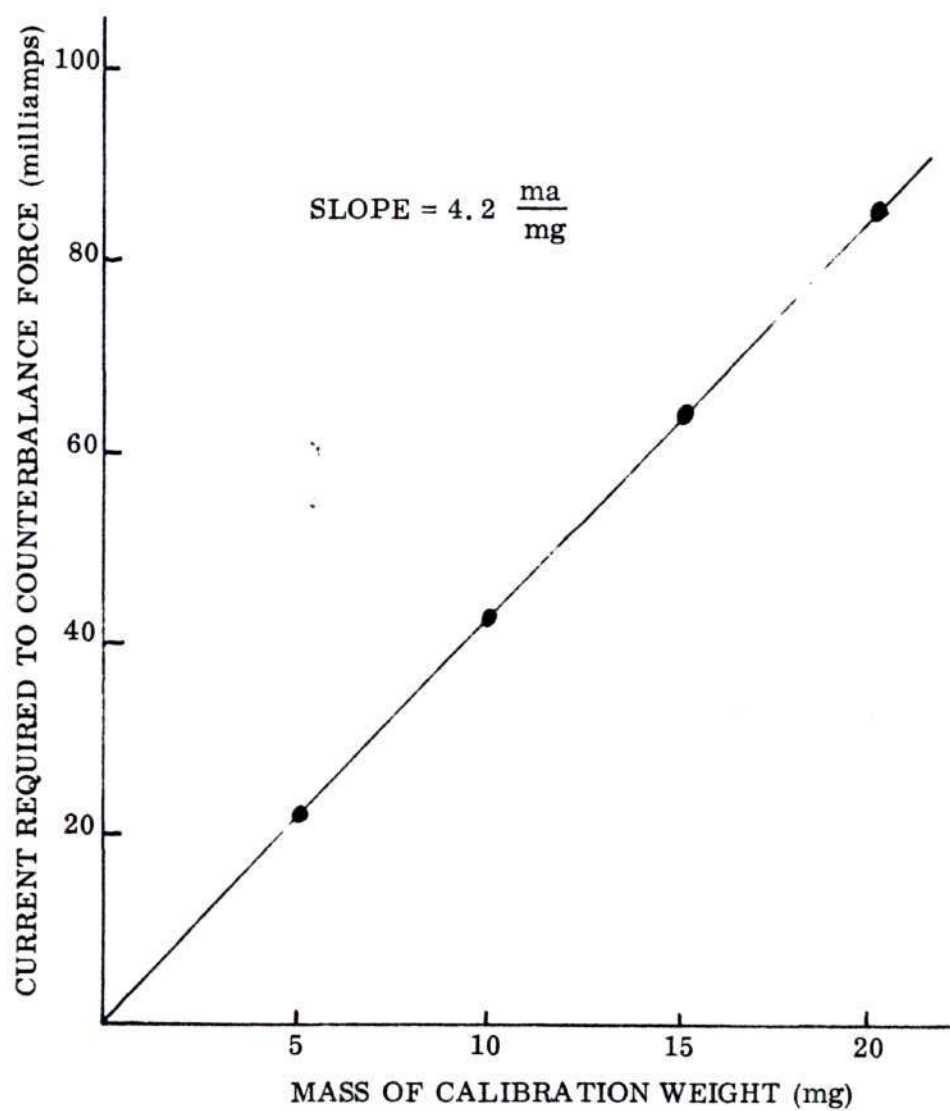


Figure 6. Calibration Data for Electrically-Operated Frictional Force Applicator.

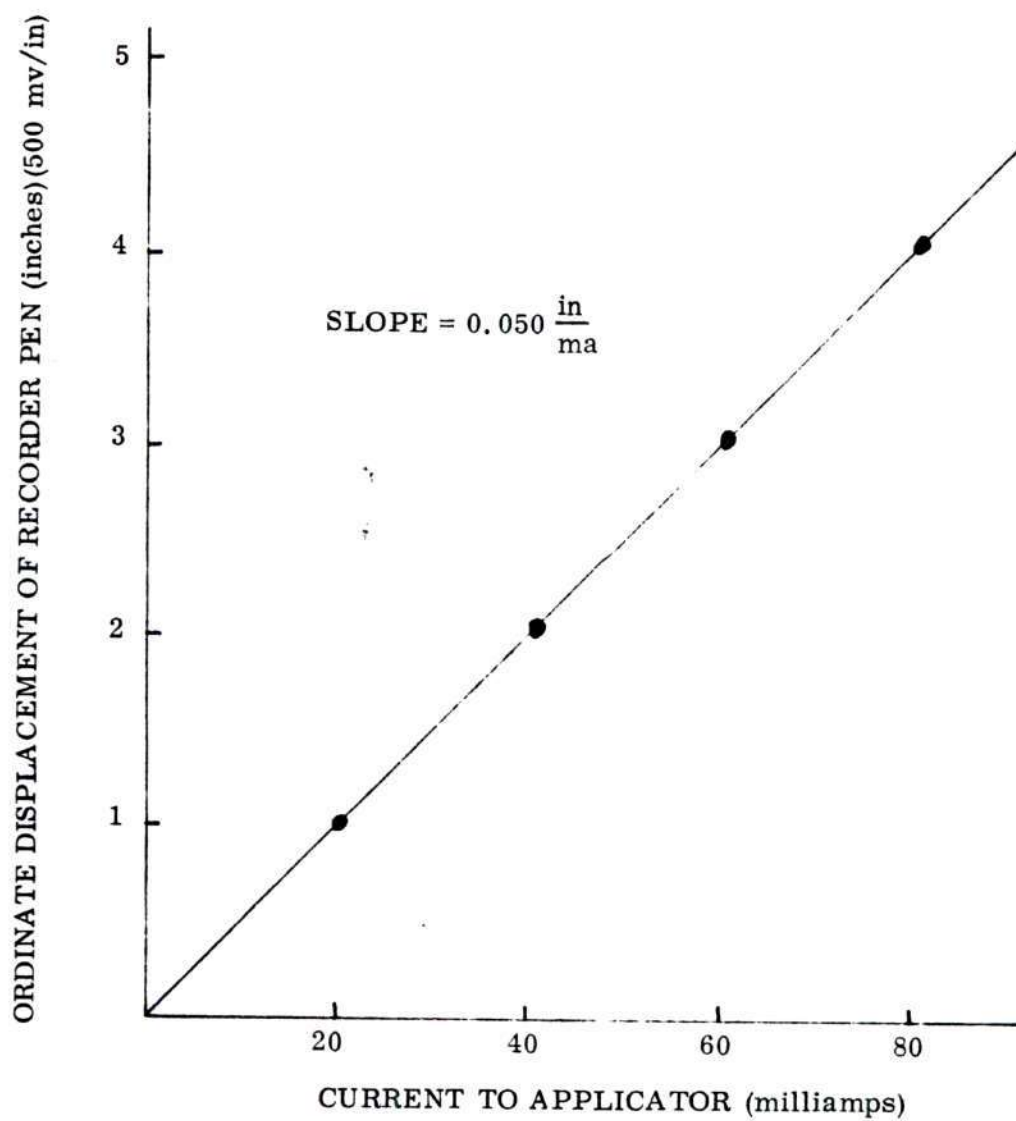


Figure 7. Calibration Data for Friction Sensing Apparatus.

Modifications

One additional refinement proved helpful in the use of the horizontal calibrator. As originally built by Huff, the calibrator was equipped with screws attached to its base; these were normally driven into the plastic housing surrounding the galvanometer when the friction sensor was calibrated. In addition to being time-consuming, this action damaged the housing unnecessarily. With the assistance of J. C. Meaders, the mounting assembly was removed from the housing and two brass bars nine inches in length were permanently attached to the base. With this improvement, the calibrator could be simply rested in a stable position on top of the plastic housing when necessary, and removed quite easily on completion of the calibration step.

Materials

The materials investigated in this study consisted of six different types of Nylon 66 which were produced by E. I. duPont de Nemours and Company. These fibers ranged in denier from 7 to 20, in shape from circular to trilobal, and in delusterant content from 0.02 to 2.0 per cent. Table 1 outlines the specifications of the various Nylon 66 fibers evaluated. Typical scanning electron micrographs which depict surface features are shown in Figures 8-14.

Nylon 66, which is often referred to as normal nylon, is made from adipic acid, $\text{COOH}(\text{CH}_2)_4\text{COOH}$ and hexamethylene diamine, $\text{NH}_2(\text{CH}_2)_6\text{NH}_2$. The polymer is referred to as "66" nylon because each of the raw materials contain six carbon atoms. Nylon 66 is a melt spun fiber.

Table 1. Specifications of Nylon 66 Fibers Investigated

Denier	Type	Finish	Cross-Sectional Shape	Per Cent Delusterant Content
7	280	semi-dull	circular	0.3
10	280	semi-dull	circular	0.3
15	280	semi-dull	circular	0.3
20	280	semi-dull	circular	0.3
15	90	bright	trilobal	0.02
15	680	dull	circular	2.0

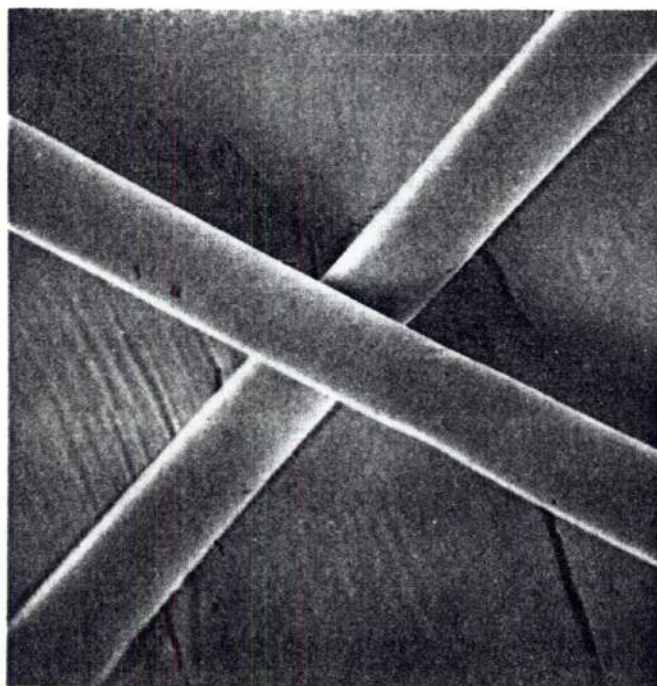


Figure 8. Scanning Electron Micrograph of Surface of 7 Denier Type 280 Nylon 66 Fiber.

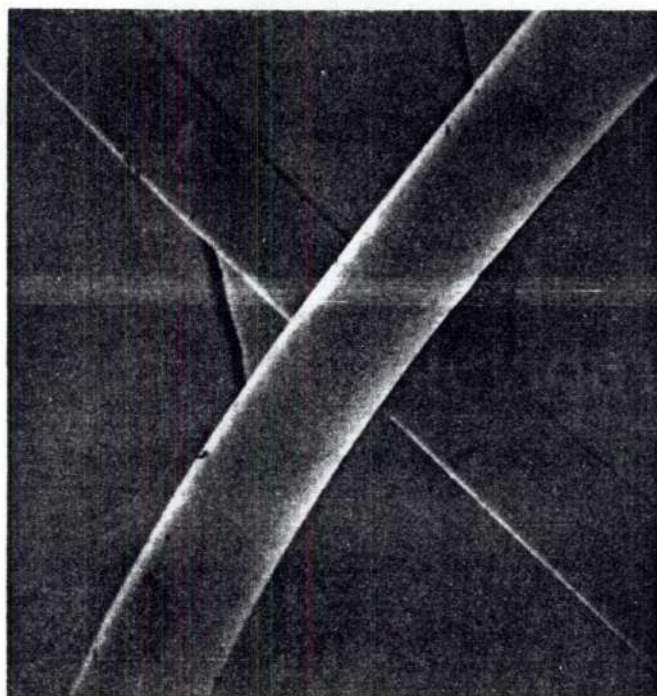


Figure 9. Scanning Electron Micrograph of Surface of 10 Denier Type 280 Nylon 66 Fiber.

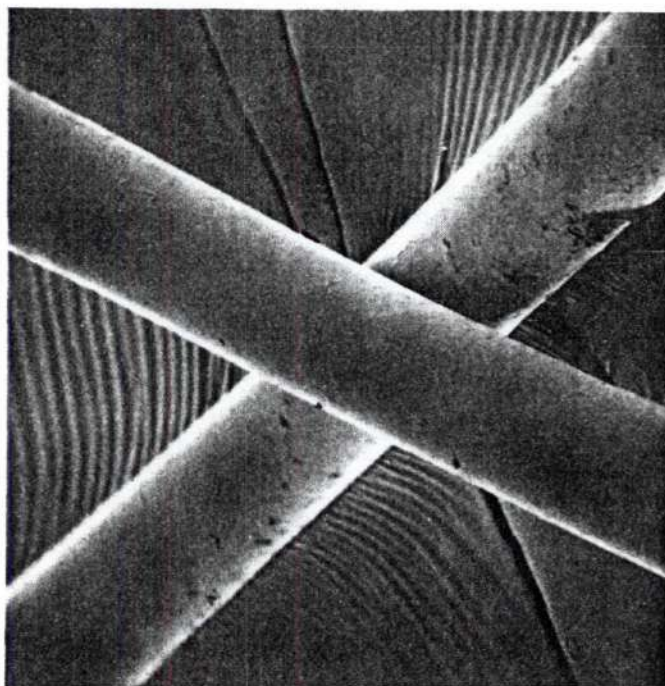


Figure 10. Scanning Electron Micrograph of Surface of 15 Denier Type 280 Nylon 66 Fiber.

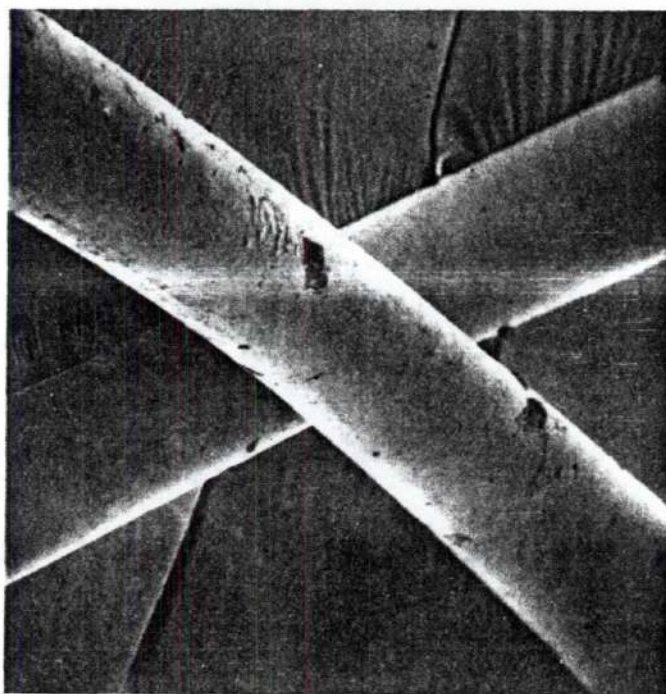


Figure 11. Scanning Electron Micrograph of Surface of 20 Denier Type 280 Nylon 66 Fiber.

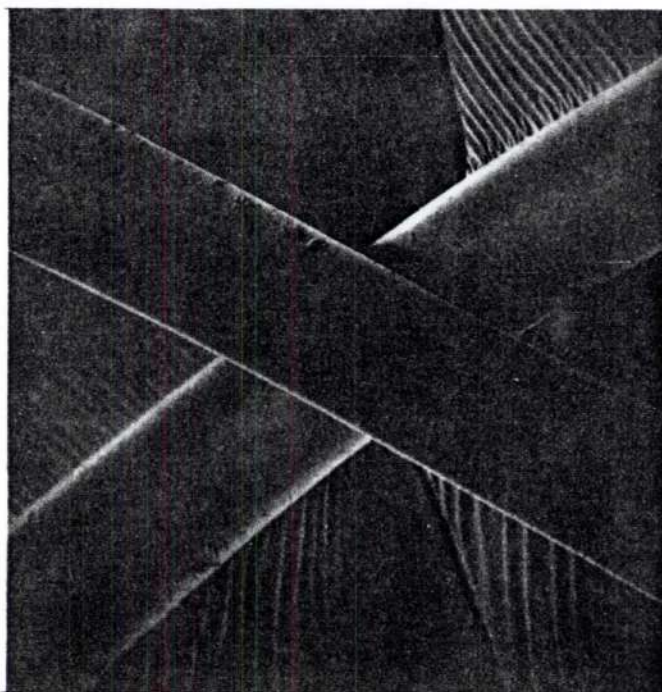


Figure 12. Scanning Electron Micrograph of Surface of 15 Denier Type 90 Nylon 66 Fiber.

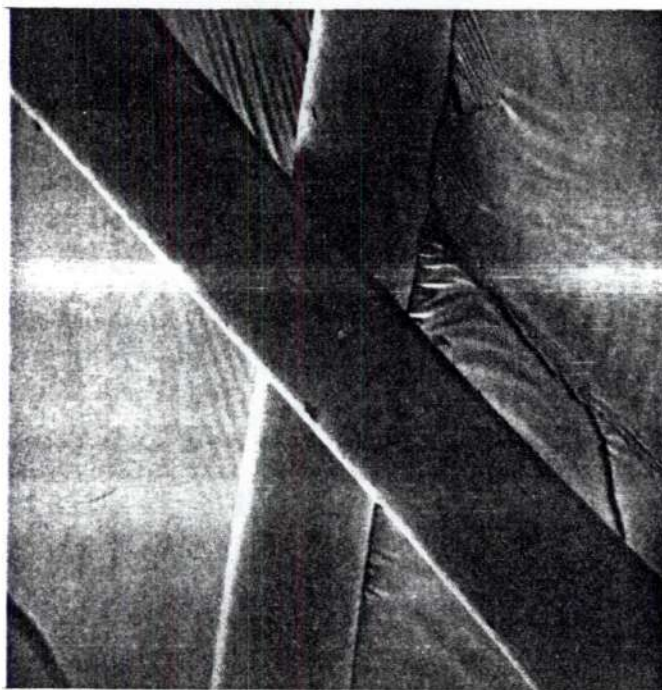


Figure 13. Scanning Electron Micrograph of Surface of 15 Denier Type 680 Nylon 66 Fiber.

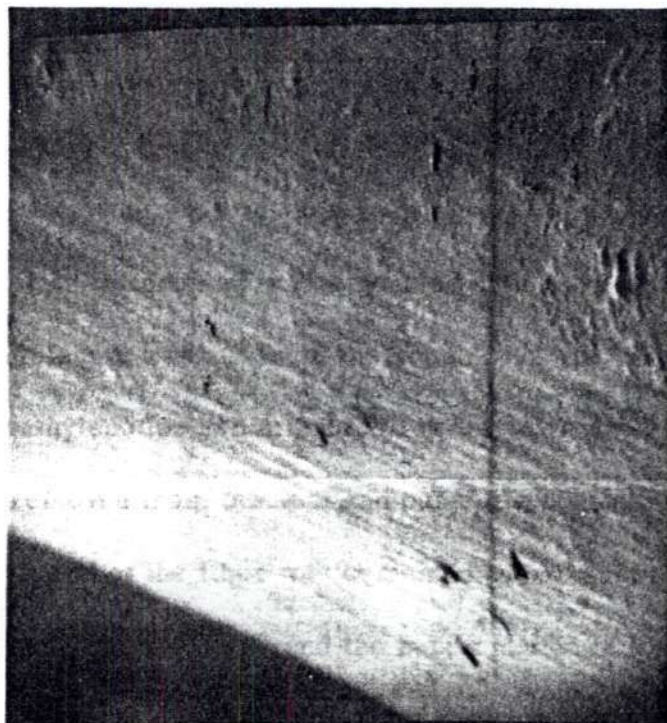


Figure 14. Scanning Electron Micrograph of Surface Features of 20 Denier Type 280 Nylon 66 (4250X).

The Nylon 66 fibers procured, except one type, exhibited circular cross-sectional shapes. The exception was the 15 denier type 90 filament, which featured a trilobal cross-section.

Measuring Procedure

Using the apparatus and fibers described in the preceding paragraphs, frictional measurements were made according to the procedure outlined below.

The fiber to be mounted on the sensing arm (lower position) was selected and a three-inch length was cut from the bobbin. It was placed in a cold bath of 1, 1, 1 trichloroethylene for two minutes in order to remove the surface finish. The fiber was removed from the bath and carefully placed on top of the lower fiber "U" mount. One end of the fiber was cemented to one arm of the mount, the cement was dried for five minutes, and the mount placed in a clamp which held its axis vertically. A 425 mg weight was glued to the free end of the fiber and another five minutes was allowed for the glue to dry. The weighted fiber was carefully positioned over the second arm and cement was applied at the fiber-arm contact zone and permitted to dry. In this manner, a reproducible tension was obtained for successive fibers. The extra length of fiber at its ends was cut away and the fiber holder with the attached fiber was cemented in an upright position at a precise location on the galvanometer needle. A second fiber, the traversing one, was glued to its holder using essentially the same method. Once the test specimens were mounted, the light source, Burr-Brown operational amplifier, X-Y recorder, and integrator were switched on and allowed to warm up for a few minutes. After the frictional stick-slip plots similar to the one illustrated in

Figure 15 had been obtained under the specified conditions, the coefficients of static and kinetic friction were calculated from the data exhibited in the respective data plots. According to Amonton's Law, frictional force equals k (some coefficient) times the normal force. If k is defined as μ , then the coefficient of friction can be expressed as follows:

$$\mu = \frac{\text{Frictional Force}}{\text{Normal Force}}$$

The average value of the ten maximum deflections from the base line of the frictional plot was arbitrarily defined as the value of the static coefficient of friction, μ_s . The deflections, or peaks viewed in the plot, represent the maximum frictional forces (sticks) experienced during the traverse of this fiber across a second. The static coefficient was calculated with the following function:

$$\mu_s = \frac{(\text{Avg. Value of 10 Max. Deflec.})(\alpha \text{ in mg/volt})(\text{Rec. Sens. in volt/in})}{\text{Normal Force in mg}}$$

The method for computation of α , which is the scale factor in mg/volt, is given in Table 4 of the appendix. For each frictional plot, μ_s was calculated on the basis of the average of all deflection peaks from the base line.

The kinetic coefficient μ_k was determined by using the following expression:

$$\mu_k = \frac{(\text{Integrator Reading in Volts})(\text{Integrator Constant})(\alpha \text{ in mg/volt})}{(\text{Timer Reading in seconds})(\text{Normal Force in mg})}$$

This value may also be obtained by use of a planimeter to find the area under the

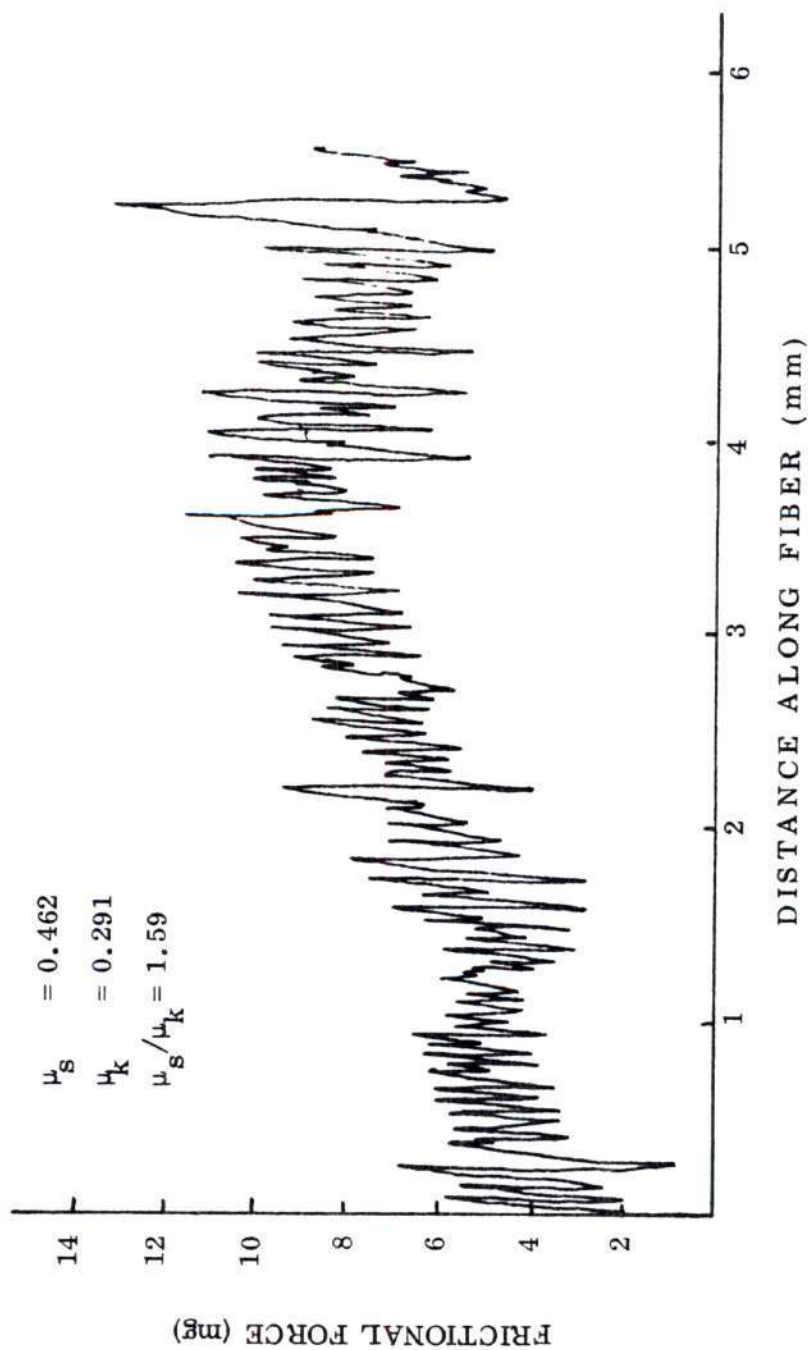


Figure 15. Typical Frictional Plot for Fiber Pair of 7 Denier Type 280 (Semi-Dull) Nylon 66 at 10 mg Normal Force.

curve which represents the average force acting over the length of fiber traversed. The calculation of the integrator constant is found in Table 5 of the Appendix. Its value was 1.72 sec. throughout the work.

Once μ_s and μ_k were determined, the ratio μ_s/μ_k could be readily computed. This latter value was of use in studying the character of the data. The character, the general pattern of the curve, is featured by such items as number of peaks per unit length, energy of the peaks as represented by the respective areas under them, the reiteration of types of sequences, and repeatability of the pattern on successive traverses of the same fiber. These features offer characterization of the fiber material, cross-sectional shape indication, surface roughness indications, and other data related to normal force employed, fiber luster, delusterant additive, and fiber velocity.

CHAPTER IV

EXPERIMENTAL WORK

General

Measurements of the static and kinetic coefficients of friction of fiber pairs of Nylon 66 were made by means of the servo-controlled frictional measuring instrument described in Chapter III. A total of 80 fiber pairs were examined. Three measurements of each fiber pair were made at two levels of normal force. The effects of fiber diameter and delusterant content on the static and kinetic coefficient of friction were evaluated.

Effects of Fiber Size and Delusterant Content

Using the measuring procedure described in Chapter III, fifteen fiber pairs of each variety described in Table 1, except Type 90, were successively mounted and measured for frictional behavior. Only five fiber pairs of the 15 denier Type 90 variety were examined. The traversing fiber (upper) of each pair was long enough to permit three separate successive measurements to be made. Consequently, the characters of essentially three different zones of each fiber could be measured using the same fiber pair. The friction of each fiber pair was measured at normal force levels of 10 and 20 mg, in that order, to minimize ploughing or other wear effects. Since each of 80 fibers were subjected to six measurements, three at each normal force, a grand total of 480 frictional plots

was obtained. Temperature and humidity conditions were not controlled but measurements indicated that temperatures of $(25 \pm 2)^{\circ}\text{C}$ and relative humidities of (60 ± 5) per cent were the condition limits experienced. Typical data obtained for the fibers of various diameters and delusterant contents are illustrated in Figures 15-20. The specific conditions for each measurement and the respective calculations are shown on each data plot. Average data for all the various experiments are listed in Table 2. Complete data are found in the Appendix in Tables 6-11. For fibers of the same cross-sectional shape and delusterant content, the values of μ_s and μ_k are observed to increase as the fiber diameter increases. This trend is observed for both normal forces employed. The data are more clearly indicated by plotting the values of μ_s , μ_k , and μ_s/μ_k against fiber denier and fiber diameter. These data are exhibited in Figures 21-24.

For semi-dull fibers (0.3 per cent TiO_2), Figures 21 and 22 show that the slopes of the lines for the variation of μ_s and μ_k versus denier or diameter are essentially constant.

Essentially one slope fits the data. The positive trend of the frictional forces with diameter is apparent. The plots of μ_s/μ_k versus denier and diameter displayed in Figures 23 and 24 are very nearly constant for a given normal force, except for a small negative slope as the diameter is increased. There is an obvious change in the ratio with normal force.

The data on coefficients of friction for the fibers of various denier and delusterant content were plotted versus normal force in Figures 25-28. Figure 25 depicts the variation of μ_s with normal force. It is observed that the data follow

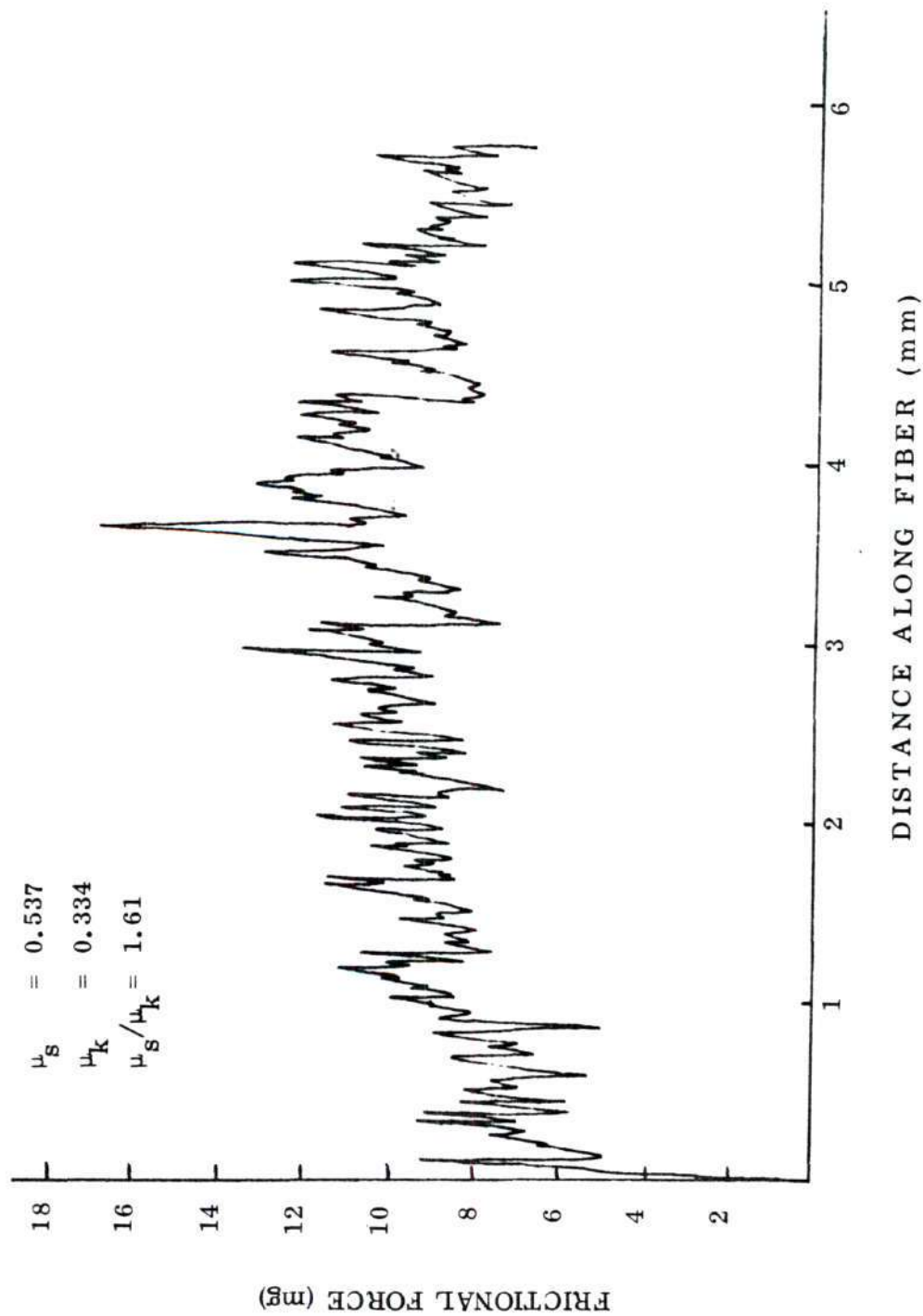


Figure 16. Typical Frictional Plot for Fiber Pair of 10 Denier Type 280 (Semi-Dull) Nylon 66 at 10 mg Normal Force.

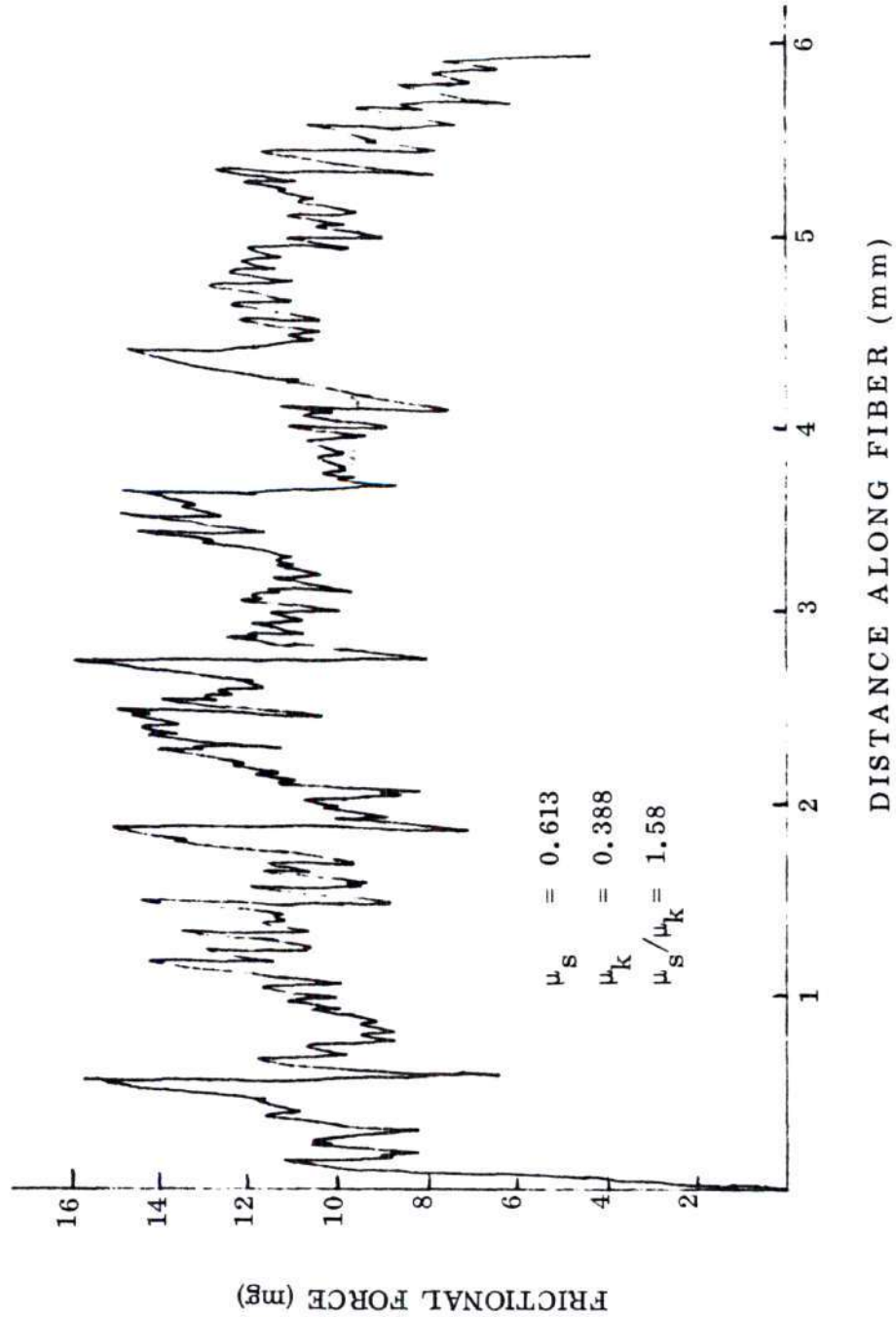


Figure 17. Typical Frictional Plot for Fiber Pair of 15 Denier Type 280 (Semi-Dull) Nylon 66 at 10 mg Normal Force.

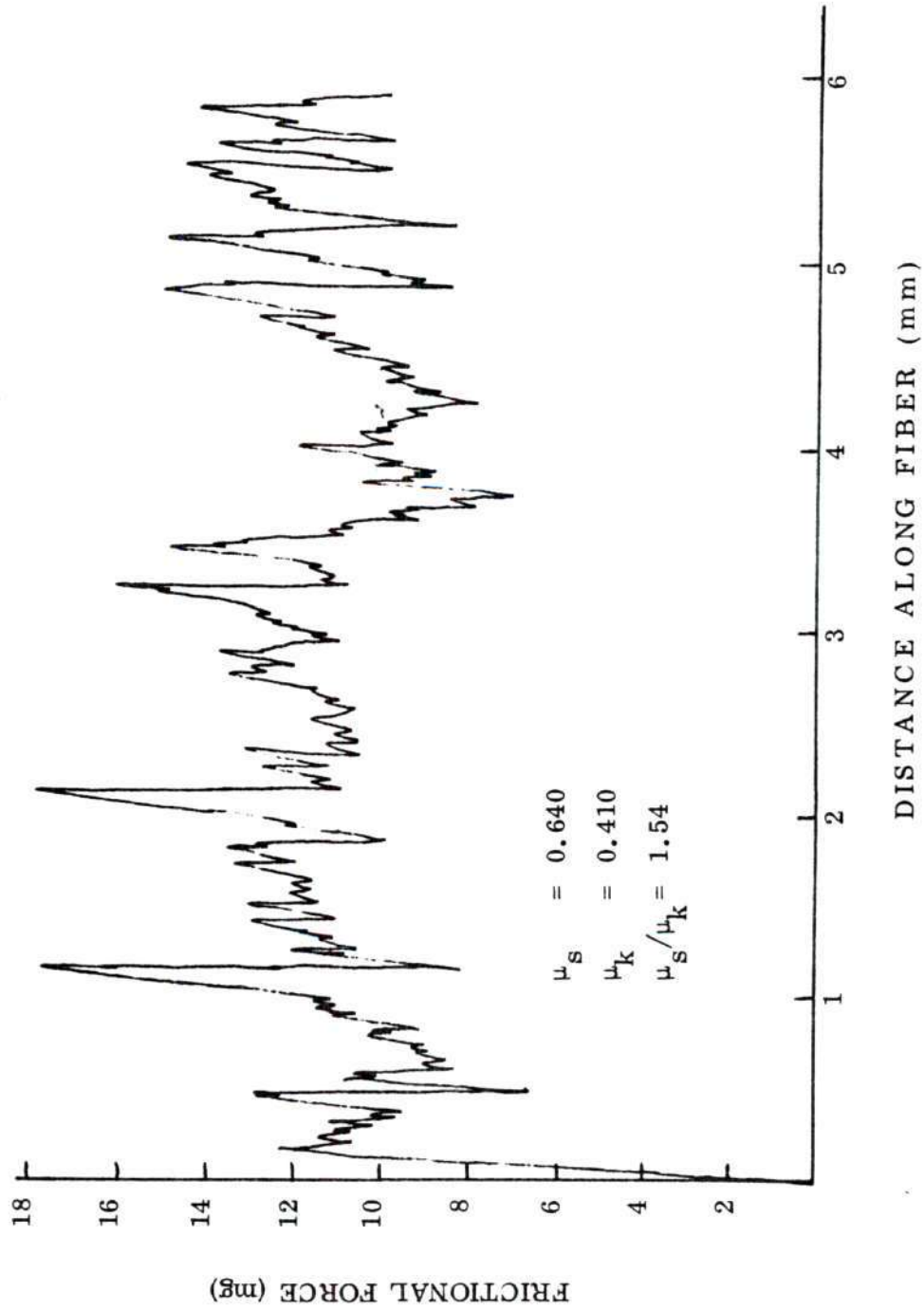


Figure 18. Typical Frictional Plot for Fiber Pair of 20 Denier Type 280 (Semi-Dull) Nylon 66 at 10 mg Normal Force.

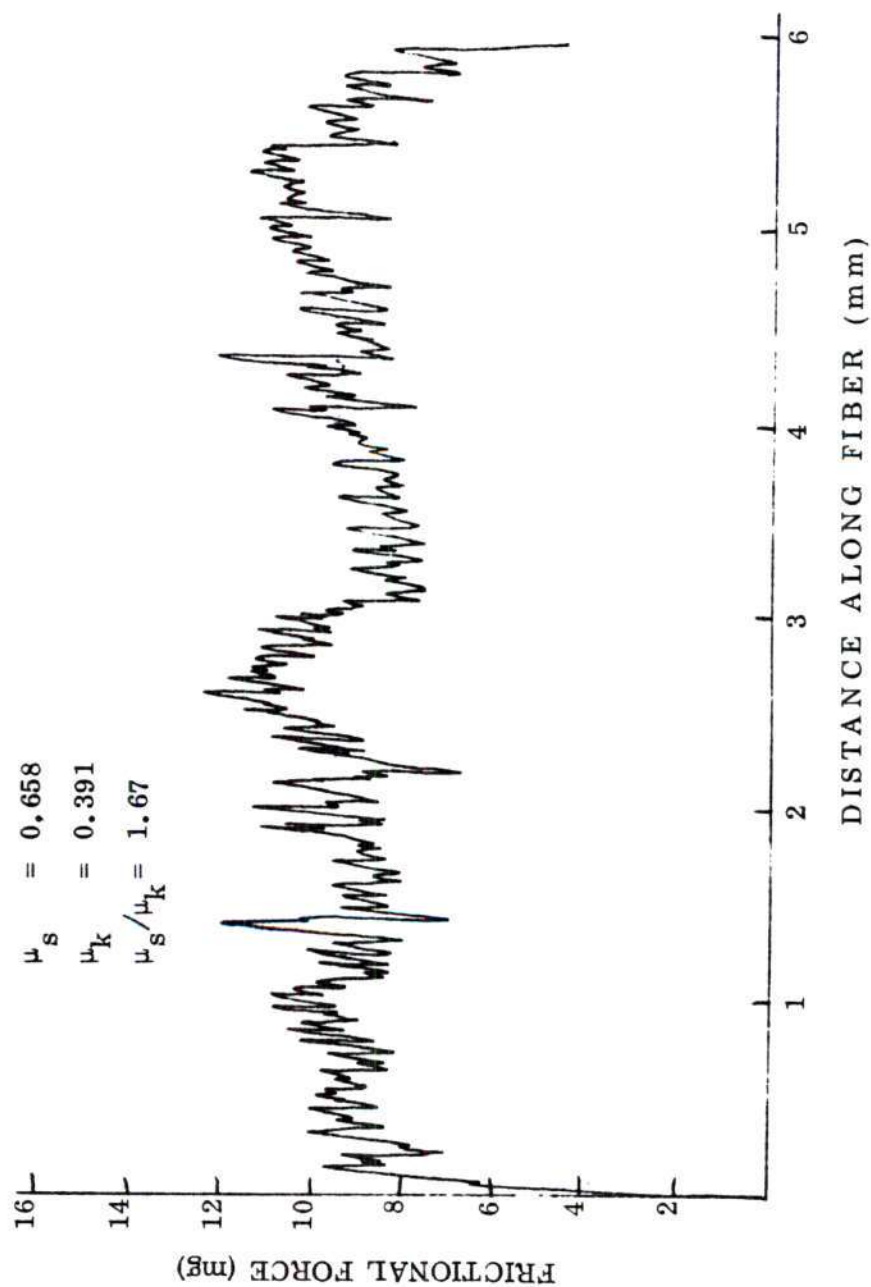


Figure 19. Typical Frictional Plot for Fiber Pair of 15 Denier Type 90 (Bright) Nylon 66 at 10 mg Normal Force.

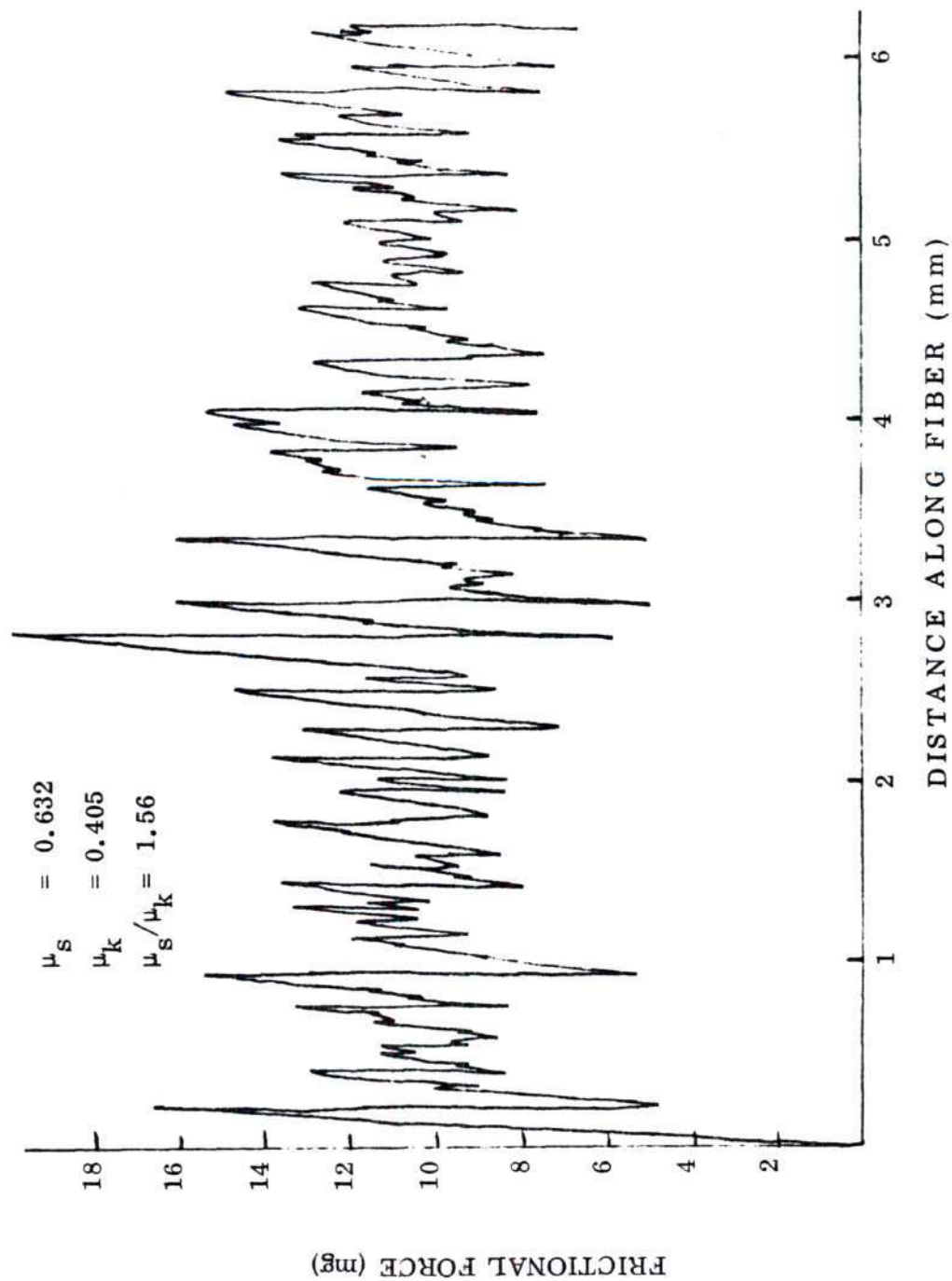


Figure 20. Typical Frictional Plot for Fiber Pair of 15 Denier Type 680 (Dull) Nylon 66 at 10 mg Normal Force.

Table 2. Data Displaying Effects of Size and Delusterant
on Friction of Nylon 66 Fibers

	10 mg			20 mg		
	μ_s	μ_k	μ_s/μ_k	μ_s	μ_k	μ_s/μ_k
7 Denier Semi-Dull	.517	.295	1.75	.456	.281	1.62
10 Denier Semi-Dull	.579	.343	1.69	.474	.299	1.58
15 Denier Semi-Dull	.611	.357	1.71	.524	.326	1.61
20 Denier Semi-Dull	.652	.398	1.64	.551	.370	1.49
15 Denier Bright (Trilobal)	.639	.385	1.65	.562	.355	1.58
15 Denier Dull	.620	.402	1.54	.544	.381	1.43

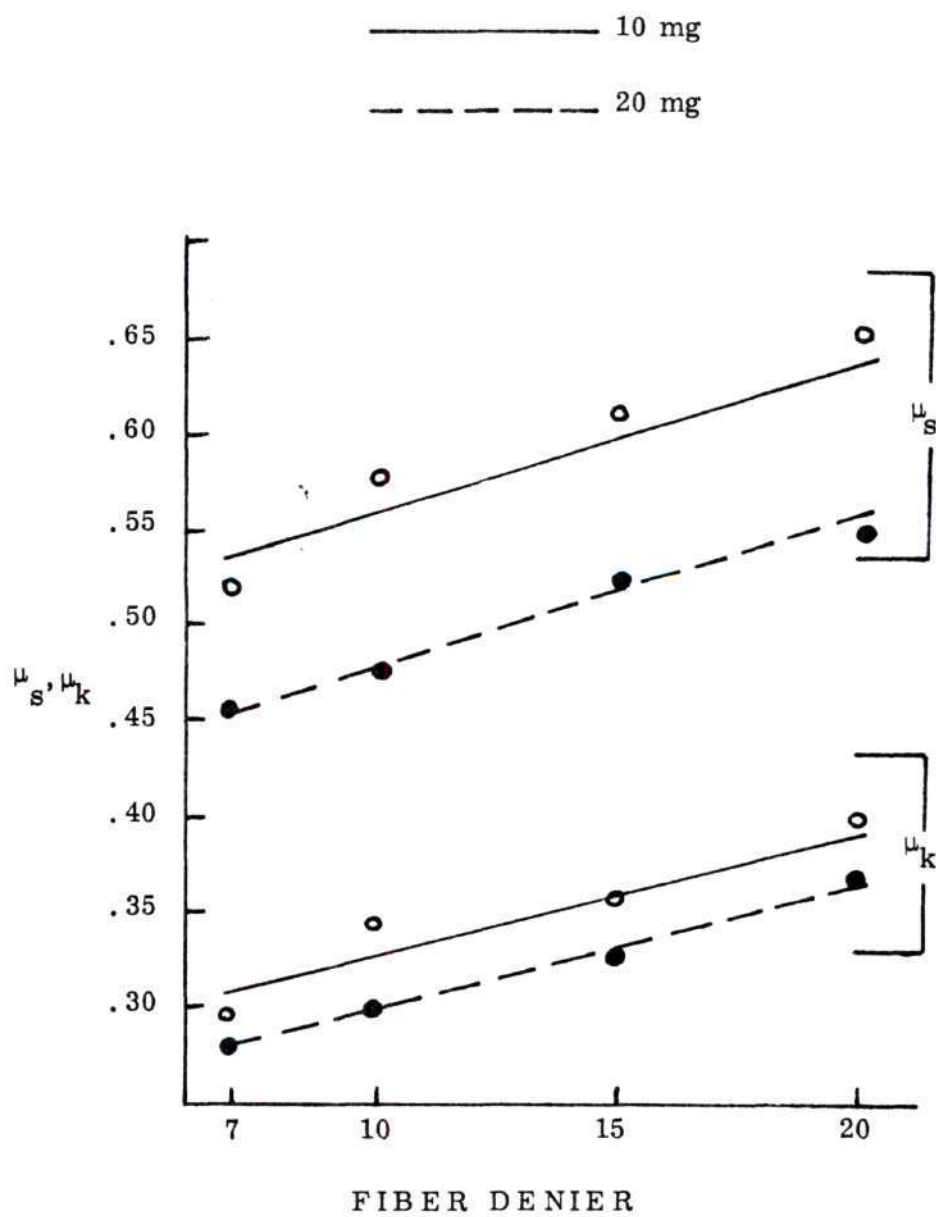


Figure 21. Variation of μ_s and μ_k with Fiber Denier for Semi-Dull Nylon 66 Fibers.

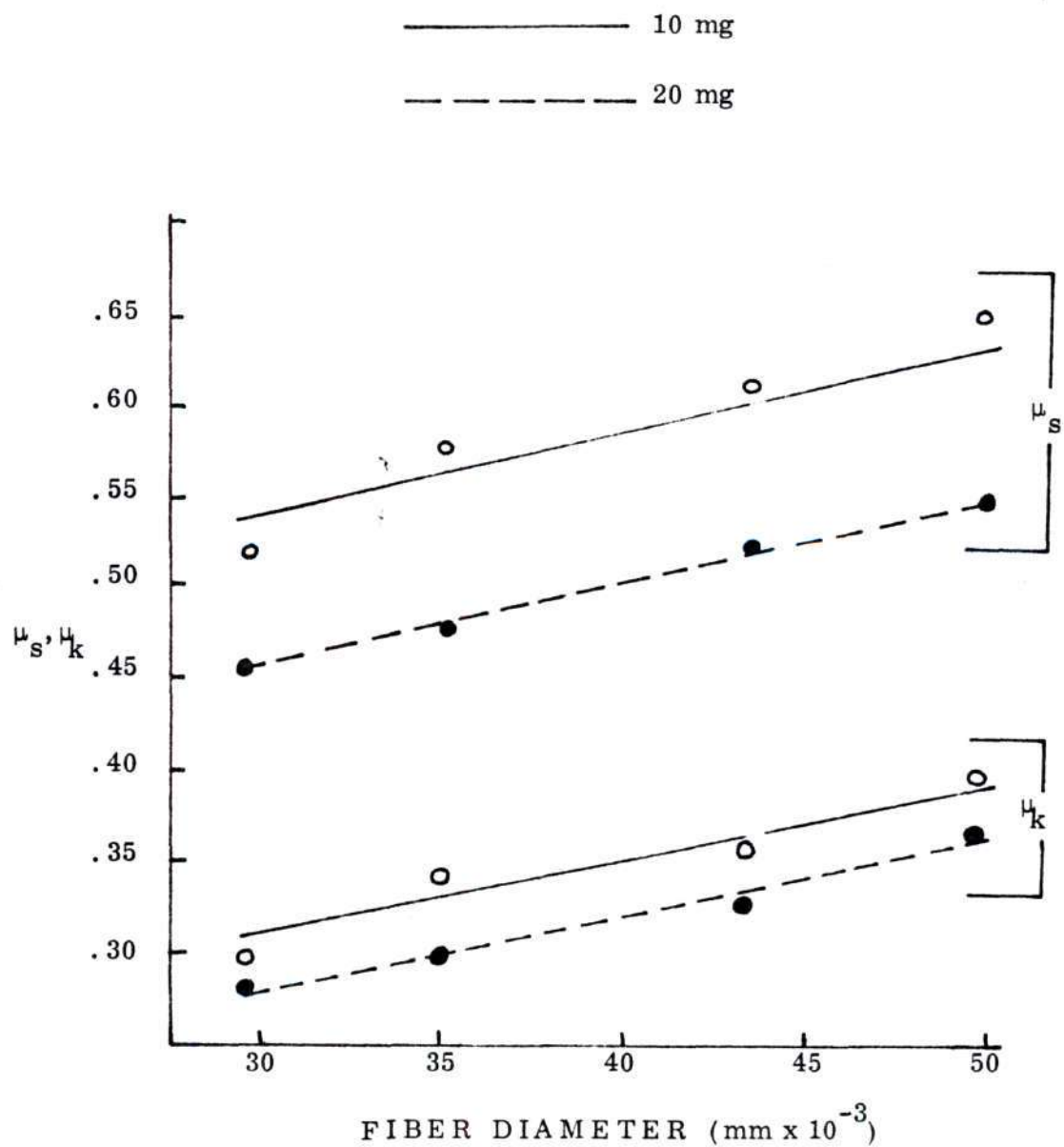


Figure 22. Variation of μ_s and μ_k with Fiber Diameter for Semi-Dull Nylon 66 Fibers.

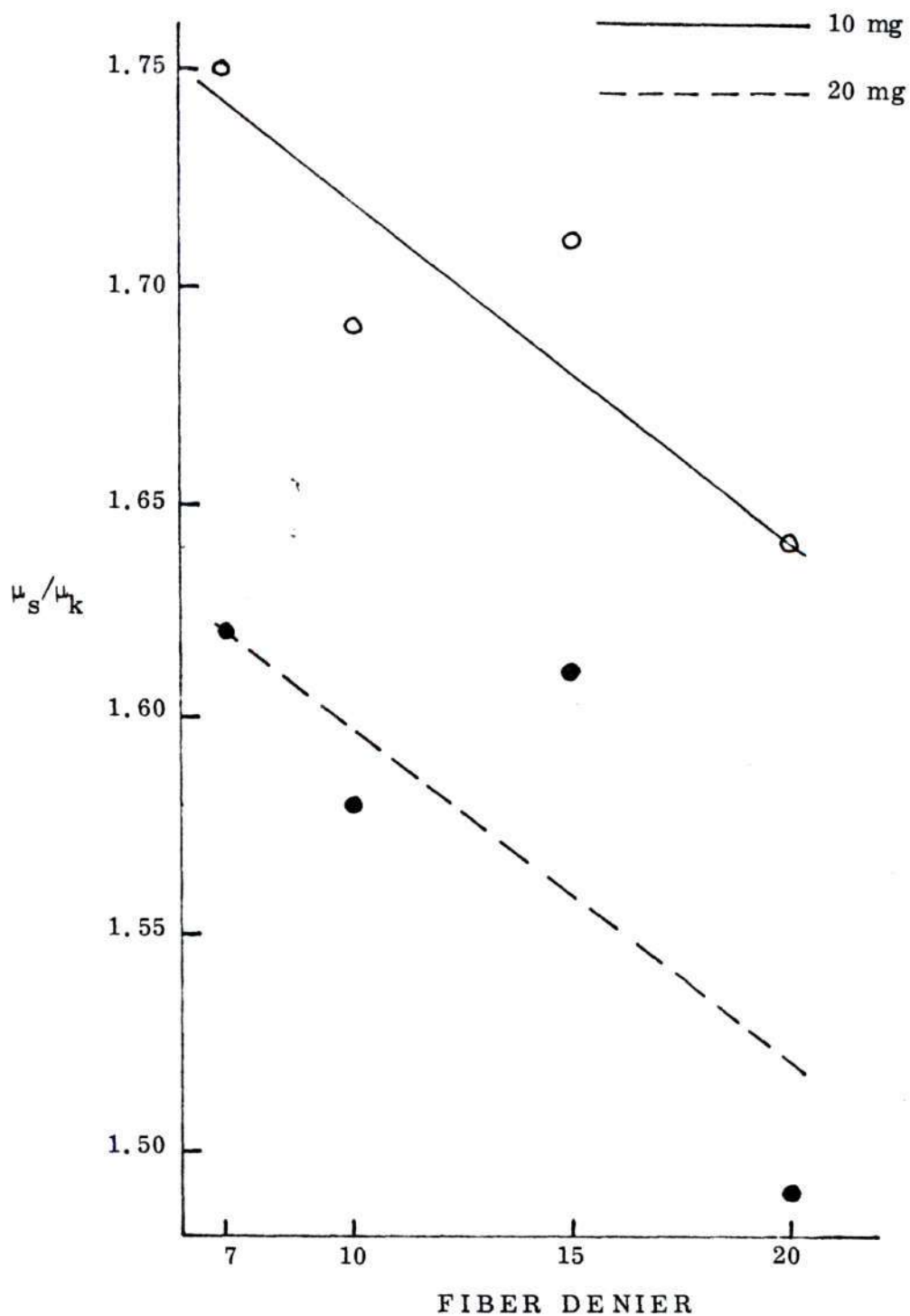


Figure 23. Variation of μ_s/μ_k with Fiber Denier for Semi-Dull Nylon 66 Fibers.

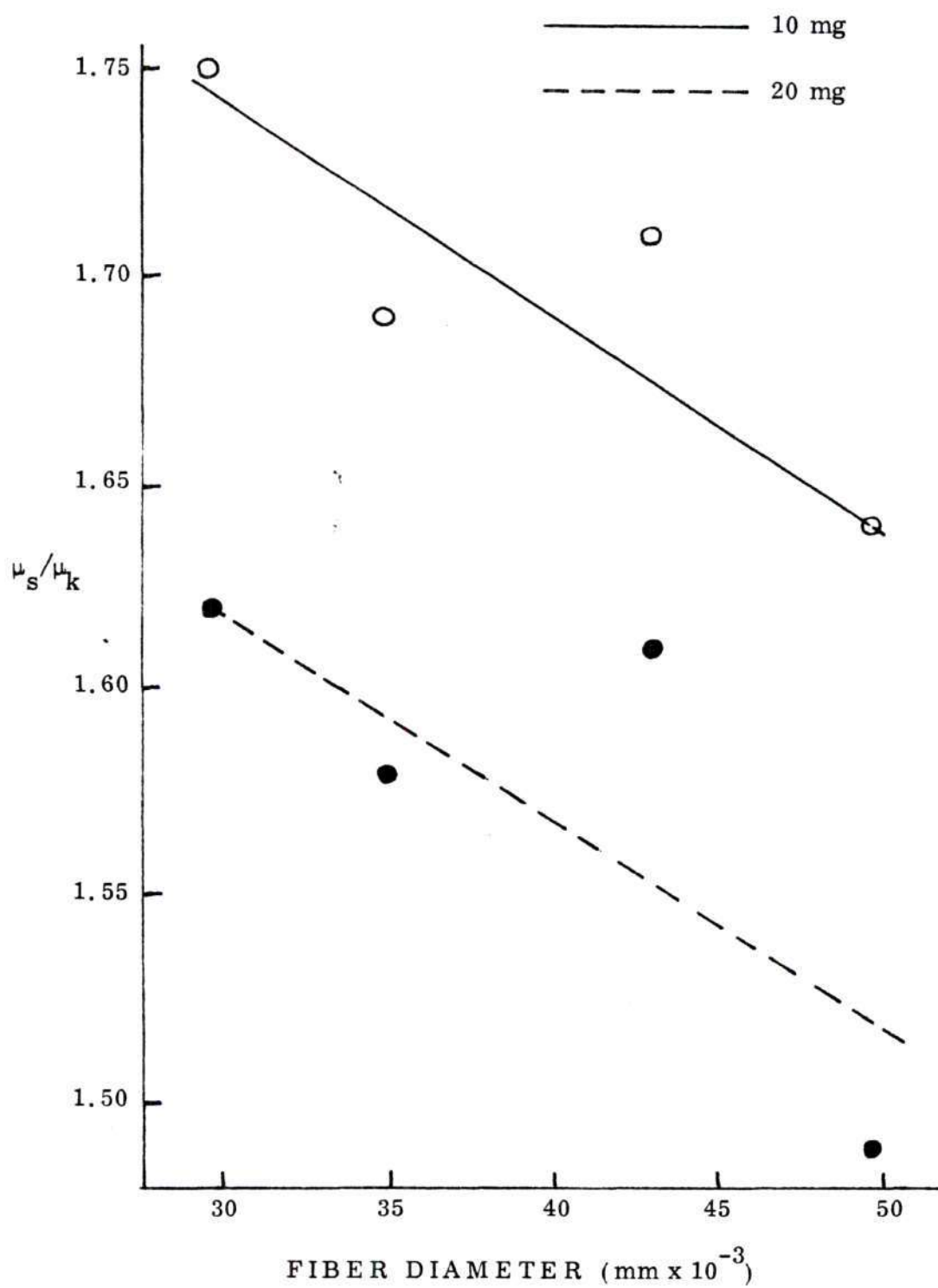


Figure 24. Variation of μ_s/μ_k with Fiber Diameter for Semi-Dull Nylon 66 Fibers.

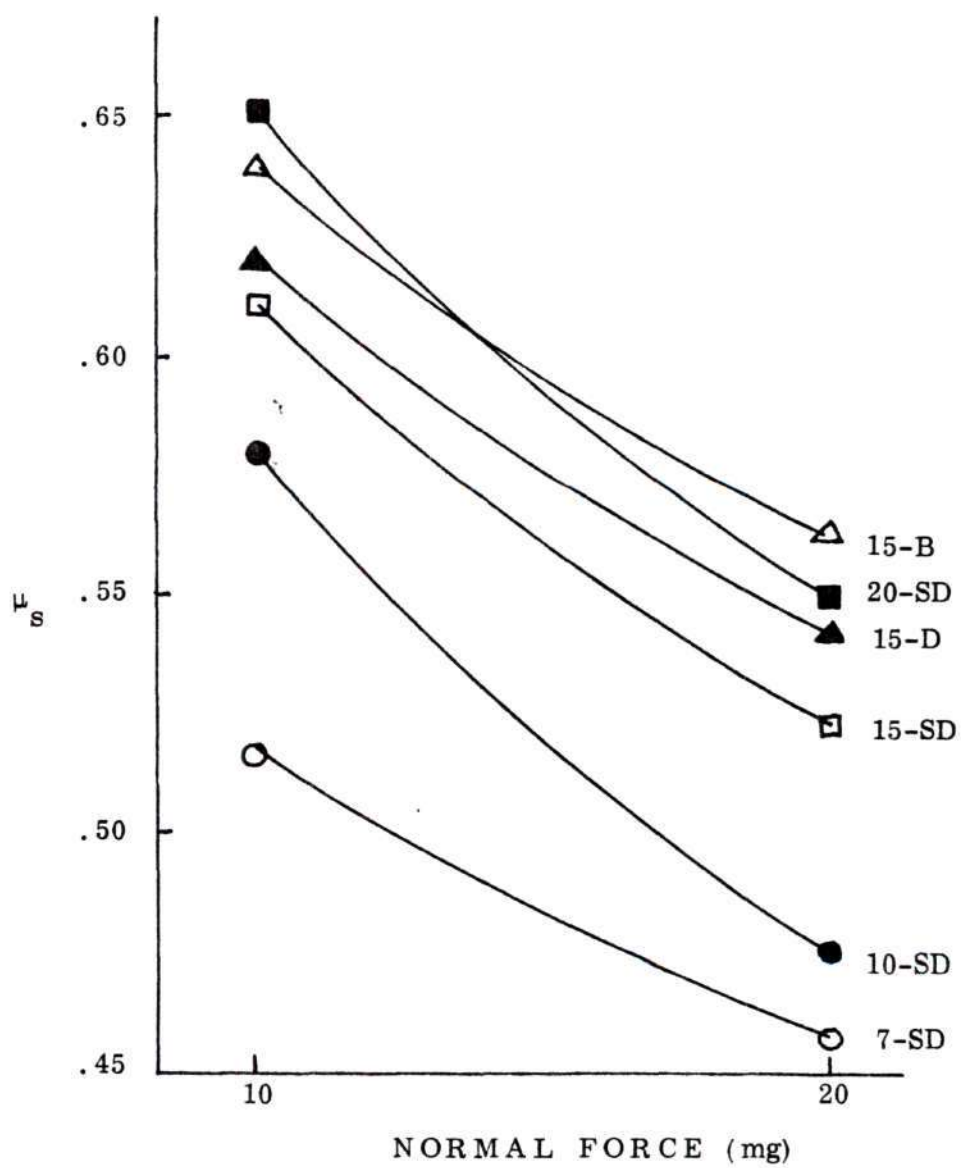


Figure 25. Variation of μ_s with Normal Force for Nylon 66 Fibers.

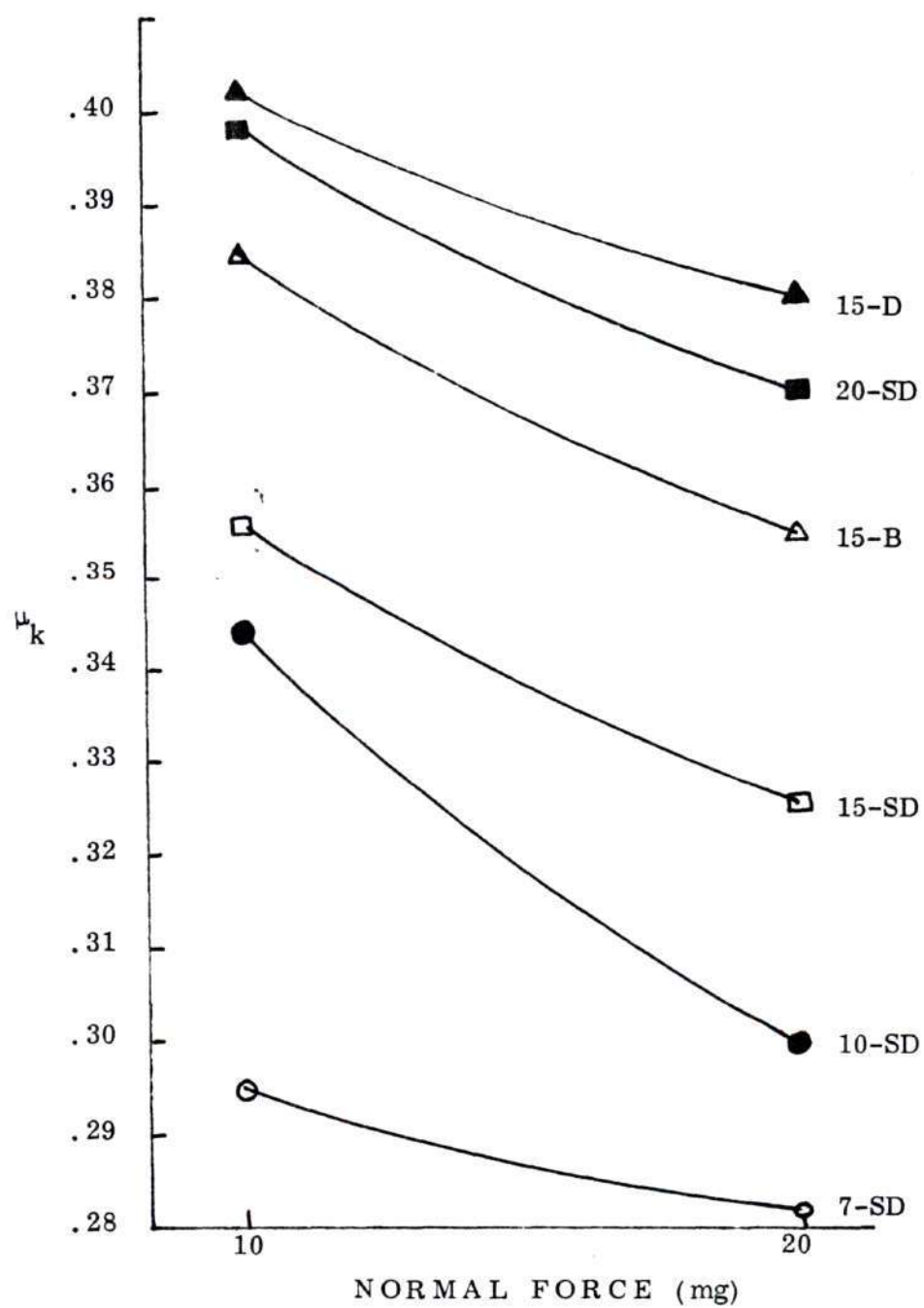


Figure 26. Variation of μ_k with Normal Force for Nylon 66 Fibers.

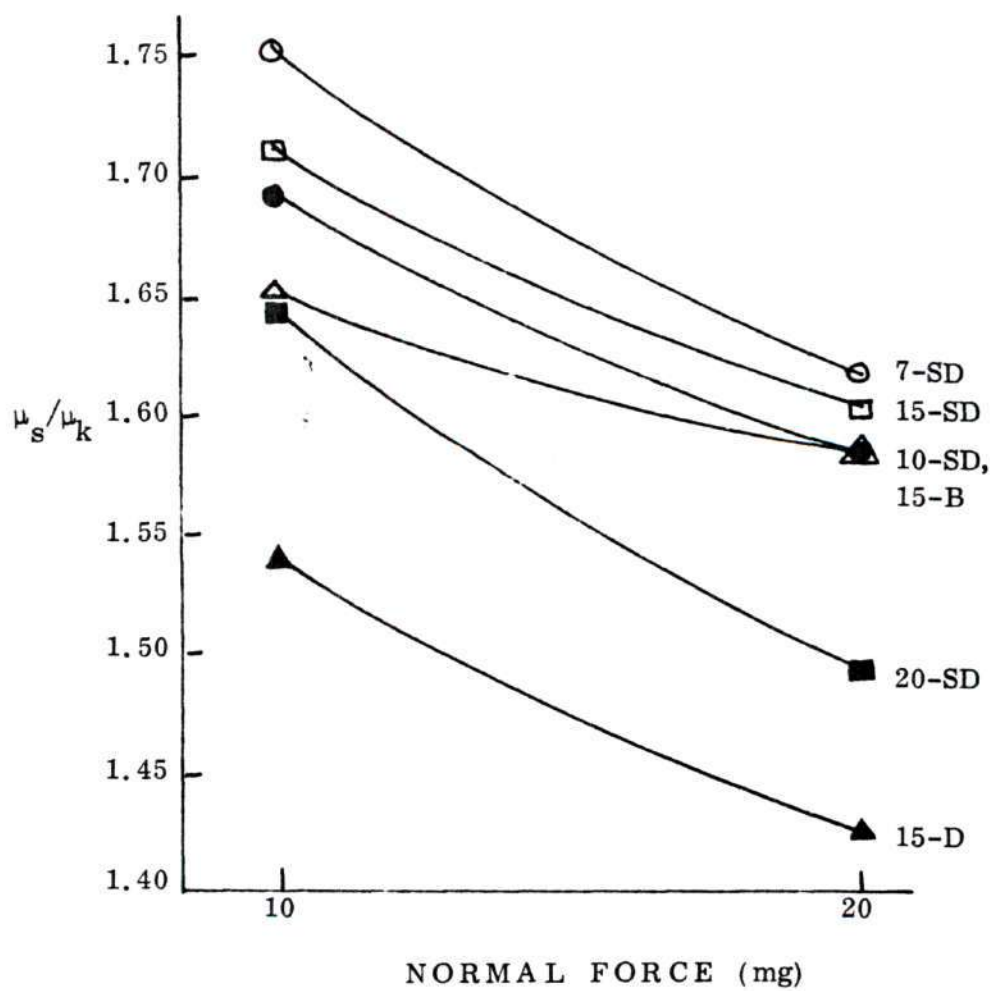


Figure 27. Variation of μ_s/μ_k with Normal Force for Nylon 66 Fibers.

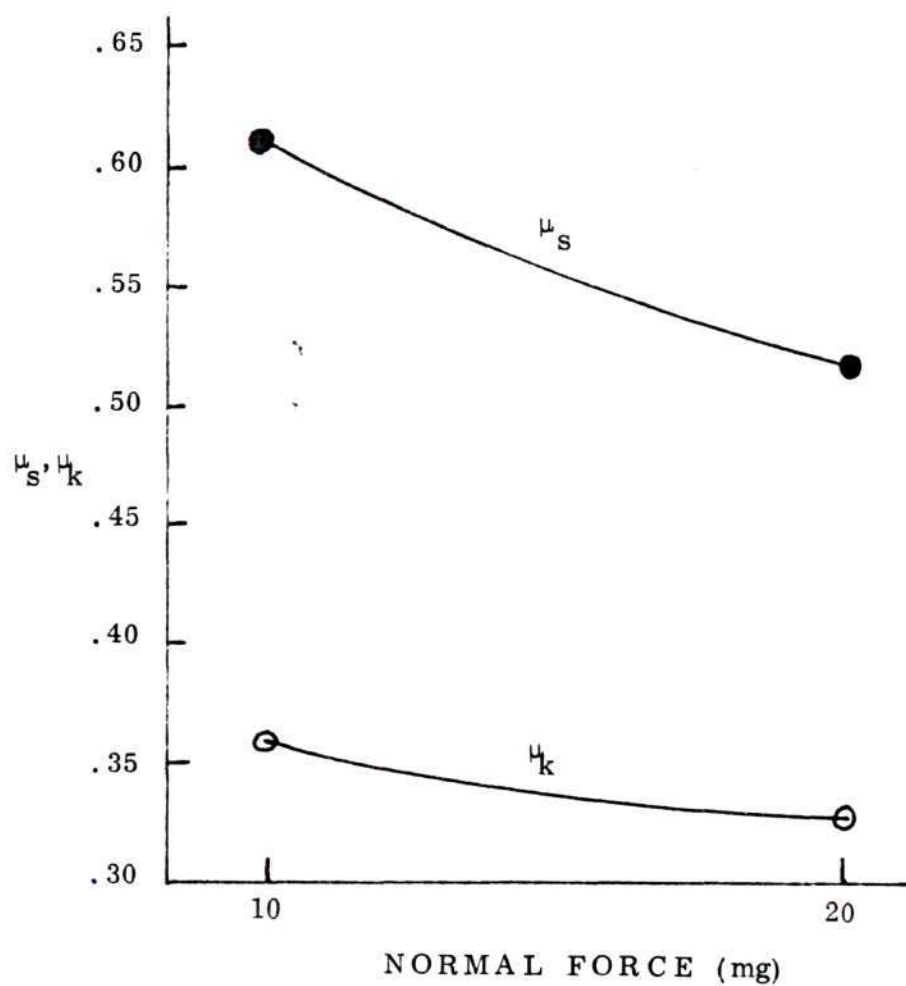


Figure 28. Comparison of μ_s and μ_k Versus Load for 15 Denier Type 280 (Semi-Dull) Nylon 66 Fibers.

the expected pattern of increase in μ_s as the normal force is decreased per data previously outlined by Pascoe and Tabor (16) and Belser and Taylor (14). The effect of denier in increasing the values is obvious. In addition, the dull and bright trilobal fibers follow essentially the same pattern at a slightly higher position on the graph.

The data also display some limited information concerning the effect of delusterant content and shape. These data are displayed in Figures 25-28 and Table 2. Considering only 15 denier fibers it is noted that both the dull and bright fibers display slightly greater coefficients of friction than the semi-dull fibers. The μ_s/μ_k ratios for the bright and dull fibers are found to be lower than for the semi-dull. Small differences in values apparently occur but the data are insufficient and the ranges of delusterant investigated are too limited for a valid conclusion. The most surprising element is the rather small difference of μ_s/μ_k observed in the behavior of the fibers of relatively large delusterant ranges.

A second method was employed for computing the coefficient of static friction (μ_s) from the frictional plot of a fiber pair. This method consisted of finding the average value of all the displacements of stick-slip peaks on the frictional plot, and was used to evaluate a typical frictional plot. The particular fiber pair analyzed was of the 15 denier Type 280 (semi-dull) variety. The frictional measurements were conducted using a load of 10 mg. The data obtained are listed in Table 3. The value of μ_s obtained using this method was considerably lower than the value computed from the average force represented by the ten highest peaks and was very close to the value of μ_k obtained with the integrator method.

Table 3. Computation of Static Friction (μ_s)
Using the Average Value of the Stick
Displacements on the Friction Plot

Nylon 66 15 Denier Type 280 (W = 10 mg)		
Displacement (inches)	Frequency	Product
0.4	1	.4
0.9	1	.9
1.0	1	1.0
1.2	1	1.2
1.3	2	2.6
1.4	4	5.6
1.5	1	1.5
1.6	4	6.4
1.7	3	5.1
1.8	8	14.4
1.9	13	24.7
2.0	7	14.0
2.1	14	29.4
2.2	11	24.2
2.3	8	18.4
2.4	14	33.6
2.5	14	35.0
2.6	14	36.4
2.7	12	32.4
2.8	15	42.0
2.9	10	29.0
3.0	12	36.0
3.1	8	24.8
3.2	5	16.0
3.3	5	16.5
3.4	2	6.8
3.5	5	17.5
3.6	3	10.8
3.7	1	3.7
3.8	1	3.8
TOTAL	200	494.1
Average Displacement = $\frac{494.1}{200} = 2.46$		
$\mu_s = \frac{(8.44 \text{ mg/volt})(0.2 \text{ volts/inch})(2.46 \text{ inches})}{10 \text{ mg}}$		
$\mu_s = .415$	$\mu_k = .388$	$\mu_s/\mu_k = 1.07$

Accordingly, this resulted in a new μ_s/μ_k ratio of 1.07. It is probable that the greatest variance would be observed in the case of the dull fibers since the peaks display fairly large energy levels, especially at 20 mg. These data confirm the accuracy of the method of Pascoe and Tabor (16) and substantiate measurements made by Huff (10).

Sources of Error

There were a number of possible sources of errors in this investigation. An important source was an integration zero effect on low normal force values. A second source of error was injected if the fiber on the sensor arm was not mounted so that the fiber, its support arms, and the galvanometer arm were in the same vertical plane. In this event, the normal force also applied a force vector affecting the friction sensor zero. A third source of error was a slight shift of the X-Y recorder base line when the sensitivity was changed. Any ordinate shift affecting the recorder zero biased the particular measurement.

DC motors are known to change speed slightly as input current varies and this fact no doubt affected fiber traverse speed to some extent. Gunther (9) showed that the speed of traverse exerted a considerable effect upon frictional values.

Other sources of error were inconsistent fiber surface finish removal, involuntary loss of tension of the fiber in the lower holder, and visual errors, especially in the placing of the lower fiber holder in an upright position. The slightest deviation of the holder from the vertical position caused the recorder pen to vary from the base line position. The calibration steps were susceptible

to error, particularly where an arm had to be visually checked for horizontal alignment. Repeatability of the measurements throughout the work, however, indicated that errors were insignificant or averaged out.

CHAPTER V

DISCUSSION OF RESULTS

Effects of Fiber Diameter and Normal Force

The primary objective of this investigation was to determine how the static and kinetic coefficients of friction vary as a function of diameter. Values for the coefficient of static friction obtained previously by others of both natural and man-made fibers have been reported as outlined in Chapter II. Experimental conditions in these investigations varied considerably and in most cases the investigators did not specify the fiber size. Few individuals appeared to be aware that fiber diameter was a factor in measurement of fiber friction and the natural fiber under study usually occurred only in limited size ranges in commonly used forms. Comparative data on friction measurements of fibers by various investigators are presented in Table 12 of the Appendix.

The expression provided by Pascoe and Tabor for variation of the coefficient of friction of fibers with fiber diameter and normal force was as follows: (16)

$$\mu = sK W^{-0.26} D^{0.52},$$

where μ = coefficient of friction, s = specific shear strength of the interface and is constant, k = a constant, W = applied load or normal force, and D = fiber diameter. In order to compare the experimental results obtained in this investigation

with those of Pascoe and Tabor, the values of the exponents x and y in the expression

$$\mu = sk W^{-y} D^x$$

were determined and compared with the x and y values obtained by Pascoe and Tabor.

Figure 22 in Chapter IV shows that the slopes of the lines displaying the variation of μ_s and μ_k with fiber diameter are approximately the same. According to the equation just discussed,

$$\frac{\mu_{k_2}}{\mu_{k_1}} = \frac{D_2^x}{D_1^x},$$

as long as W and the shear constant are maintained the same. Figure 22 was used to give a value of x equal to 0.58 for μ_k at 10 mg. Similarly, all values of x for all data were calculated and the following data obtained:

Values of x

<u>W</u>	<u>μ_s</u>	<u>μ_k</u>
10 mg	0.43	0.58
20 mg	0.36	0.60
Average	0.40	0.59

The value of x obtained by Pascoe and Tabor is nearest to that obtained here for μ_k at 10 mg. It is also evident from previous discussion by Huff (10) and Table 3

that the μ_k value here is nearest to Pascoe and Tabor's μ value since they used all stick valves in their computation.

The data revealed that because of the linearity of the plots and the similarities of slopes, a simple linear equation using the slope formula may give a better interpretation of the data over the range of diameters investigated. The formula for a line,

$$y = mx + b,$$

furnished a value of m equal to approximately 5. Hence $\mu_2 = \mu_1 + 5(D_2 - D_1)$, where D is expressed in $\text{mm} \times 10^{-3}$. If D is in microns, the same expression applies with the slope equal to 0.005. If D is in denier, m is equal to 0.0077 and $\mu_2 = \mu_1 + 0.0077 (\text{denier}_2 - \text{denier}_1)$ for a density of 1.30 gms/cm^3 .

It is possible to devise from the work of Pascoe and Tabor a value for the slope m for a $\log \mu$ versus $\log W$ plot over a large range where

$$D^x = D^{-2} \frac{(2-m)}{m}.$$

Referring to the value $x = 0.58$, $m = 2.83$ for μ_k and 2.51 for μ_s . These are in reasonable agreement with the value 2.7 given by Pascoe and Tabor. The value of μ_k is the more realistic value since μ_s as defined here and by Belser and Taylor (14) is a special case.

From

$$\mu = s k W^{-y} D^x,$$

it is seen that

$$\frac{F_2}{F_1} = \left(\frac{W_2}{W_1} \right)^{-y}.$$

Examining the data for the 15 denier semi-dull fiber, for which most data have been found by others including Huff (10) and Gunther (9), y has a value of 0.25 for μ_s . The following data were obtained in similar fashion:

<u>Fiber Type</u>	<u>y for μ_s</u>	<u>y for μ_k</u>
7 denier, 280	0.18	0.21
10 denier, 280	0.24	0.20
15 denier, 280	0.25	0.18
15 denier, 680	0.22	0.19
15 denier, 90	0.15	0.17
20 denier, 280	0.23	0.20

The large errors involved in dealing with such a short range of normal force did not allow an accurate determination of y and it is likely that the values obtained for μ_s and μ_k were different. However, averaging the values of y for the semi-dull series furnished a y value of 0.21 which is fairly close to Pascoe and Tabor's value. Hence, the formula of Pascoe and Tabor may be rewritten as

$$\mu = s k W^{-0.21}_D^{0.59}.$$

Effect of Delusterant

From the data depicted in Figures 25 and 26 and discussed in the preceding pages it is evident that there was some effect of the delusterant but this was not

exceptionally large. Although the 15 denier bright showed a higher μ_s value than either the dull or semi-dull at 20 mg, it showed a lower value than the 20 denier semi-dull at 10 mg. This may have been a shape effect superimposed upon it. As a result the y value for μ_s was low for it, 0.15 compared to 0.22 and 0.25 for the dull and semi-dull respectively. For μ_k measurements made on 15 denier fiber at 10 and 20 mg, the ascending order was semi-dull, bright, and dull.

In general, it may be said that there were small differences in the data obtained due to delusterant content, but that insufficient data were obtained to properly evaluate the effect of variation of this parameter. An additional investigation of the variation of the coefficients of friction of fibers with variation of delusterant content appears merited.

Belser and Taylor (14) proposed that smooth cylindrical fibers give large contact areas and that rougher fibers with less area and time of contact during fiber traverse would display reduced frictional forces. The reason for this apparent discrepancy was not clear. The electron scanning photomicrographs (Figures 8-14) revealed only slight differences in the surface roughness among the dull, semi-dull, and bright varieties. These micrographs were taken before frictional measurements were conducted so it was not possible to see if crevices had developed in the fibers after the successive frictional traverses.

The 15 denier bright variety of Nylon 66 of a trilobal shape produced frictional data which agreed with the data of Huff (10). In several measurements, the bright fibers (those containing the least amount of TiO_2) produced the highest static and kinetic frictional coefficients of the three types of fibers. This would appear

to confirm Belser and Taylor's observation concerning the bright fiber. However, since a shape factor was superimposed upon the size factor, i.e., the 15 denier bright variety of Nylon 66 was trilobal in cross-section, the interpretation of its behavior does not necessarily apply in the delusterant comparison.

Huff (10) found that trilobal fibers give generally lower frictional coefficients, both μ_s and μ_k , than do cylindrical fibers. This may be partially the result of a smaller area of contact between the two fiber surfaces. A second possibility proposed by Huff was discontinuous contact of the fibers during the slip phase, resulting in a considerable length of the fiber traversing without contact, hence a reduced time of contact during a traverse. It might be reasoned therefore that had the bright type of Nylon 66 fiber been circular in cross section, the μ_s and μ_k values would have been much greater.

One of the outstanding capabilities of the instrument used was its ability to display character in each curve; character is defined as a repeatable pattern observed in the analog plot of similar fibers. It is worthwhile to compare the characters of representative curves, as shown in Figures 15-20. Figures 19 and 20 reveal that there are many more short-duration stick-slip cycles for 15 denier bright fibers than for the corresponding dull fibers. Figures 15-18, which depict curves of semi-dull fibers, show stick-slip cycles of medium duration. These observations are in accord with Scheier and Lyons' findings (19) that the chart recordings for 2 denier bright Dacron (0.1 per cent TiO_2) showed more short-duration cycles than did those for dull (2.0 per cent TiO_2).

Because different recorder sensitivities were employed for measurements

at each normal force, an accurate comparison of average peak heights at each load is not possible. The 10 mg measurements exhibited sharper, taller peaks, while the 20 mg measurements displayed shorter, more blunt peaks.

Figures 15-18 reveal an increasing average peak height as the semi-dull fibers become larger in diameter. The average peak energy also appears to increase as the semi-dull fibers become larger. Figure 20, displaying data for the dull fiber, shows that energy absorption peaks exist at high loads for fibers with considerable delusterant content. Conversely, the bright fiber (Figure 19) exhibits peaks of less energy than the others.

As stated in Chapter IV and shown in Table 3, the values of μ_s obtained by measuring all peak heights and averaging them approaches the value obtained for μ_k and the ratio μ_s/μ_k approaches 1. Huff (10) reported similarly low ratios of μ_s/μ_k by this method. It appears that the data have been integrated by the method of small slices resulting in essentially the same numerical value for μ_s as that obtained with the integrator for μ_k . Hence the data of Pascoe and Tabor for μ_s on smooth fibers must approach the value we obtained as μ_k .

However, in the case of rough fibers, a greater departure of the ratio μ_s/μ_k from unity might be expected since many high energy large peaks occur at a lower frequency. Cotton fibers present an example of high energy low frequency peaks as noted by Belser and Taylor (14).

Statistical Evaluation

The data obtained relating the variation of the coefficients of static and kinetic friction to variations in fiber diameter have been analyzed statistically.

The results of this analysis are summarized in Tables 13-16, found in the Appendix. A statistical evaluation was not conducted on the data from measurements of the 15 denier trilobal fibers due to the relatively small number of tests made on this variety.

Samples consisting of five measurements of μ_k and μ_s were selected at random from each of the fiber varieties studied, with the exception of the 15 denier trilobal variety. The samples were selected from measurements made at normal forces of 10 mg and 20 mg, and were analyzed at each of these normal force levels.

The variance ratio, or F test as it is more commonly referred to, was computed for the sample data and compared to critical values found in statistical tables. The results indicated that the differences in both the μ_s and μ_k data taken at normal forces of 10 and 20 mg for different diameters of Nylon 66 fibers are significant at the 95 per cent confidence level. This implies that the values obtained for μ_s and μ_k at normal forces of 10 and 20 mg and the differences in frictional behavior observed among fibers of different diameters are real and not due to a chance occurrence of the data.

The increases in friction with fiber diameter observed are real and calculable by use of either of the formulas discussed. For limited ranges of diameter the slope formula appears simpler and more applicable. Similarly the increase in the frictional coefficient as normal force is reduced is real and fits the expression $\mu = sk W^{-0.21} D^{0.56}$. Additional measurements without delusterant or at a very low level of delusterant would undoubtedly provide statistical data at a

greater confidence level. The fibers should be of circular cross section only for proper comparisons.

CHAPTER VI

CONCLUSIONS AND RECOMMENDATIONS

Conclusions

The friction between nylon fibers in the range 7 to 20 denier and at load levels of 10 mg and 20 mg was found to follow essentially the form of the equation proposed by Pascoe and Tabor of

$$\mu = sk W^{-0.26} D^{0.52},$$

where the value μ represented a value calculated from all the sticks of the stick-slip motion and over a very wide range of normal force and fiber diameters.

Over the more restricted range measured in this research the values of

$$\mu = sk W^{-0.21} D^{0.59}$$

and

$$\mu_s = sk W^{-0.25} D^{0.40}$$

were obtained where μ_k was determined by measuring the average force from the integral of the analog frictional plot over the fiber traverse distance. The average force for μ_s was obtained from the average of the highest ten sticks of the plot.

Variations from the expression proposed by Pascoe and Tabor were contributed to the relatively short ranges of forces and diameters investigated, the

method of determining μ_k and μ_s , and the different instrumental methods employed. The validity of the s, k values with respect to these data were unknown.

A better method of determining μ_k or μ_s for fibers of various diameters over a limited range of applied loads appeared to be the slope formula. The following relation was determined:

$$\mu_2 = \mu_1 + 0.005 (D_2 - D_1)$$

where $D_2 - D_1$ is in microns; or

$$\mu_2 = \mu_1 + 0.0077 (\text{Denier}_2 - \text{Denier}_1),$$

for a fiber of density 1.30 gm/cm^3 .

The delusterant variation from 0.02 per cent to 0.3 per cent to 2.0 per cent exhibited only small effects. The data were confused somewhat by the trilobal section of the bright (0.02 per cent TiO_2) fiber and the measurement of only a single type (15 denier) of dull (2.0 per cent TiO_2) fiber. Scanning electron micrographs of fibers did not display large disparities in surface condition. More data are required for a proper evaluation of the effects on fiber friction of delusterant content. Some difference in character of the frictional data curves at 20 mg suggested ploughing and snagging of the dull fiber at this load level, presenting a data plot somewhat resembling that of an irregularly shaped fiber such as cotton.

Recommendations

Further work should be undertaken with the present instrument using bright

fibers (containing no titanium dioxide delusterant) and a greater denier range, especially below 7 denier. It might also be helpful to examine fibers with an even greater TiO_2 content than 2 per cent. A further step would be to conduct measurements using the single fiber-bundle withdrawal technique discussed by Belser and Taylor (14). Additional modifications of the present friction-measuring instrument should be made, particularly a faster method of mounting the fibers. Finally, it is possible that a frictional plot analysis, based on all the deflections to determine μ_s , made for various delusterant levels and for various shapes would provide significant information about fiber friction. Such a study is recommended.

APPENDIX

Table 4. Calculation of Scale Factor " α "

$$\text{Slope} = 4.2 \frac{\text{ma}}{\text{mg}} \quad (\text{From Figure 6})$$

$$500 \frac{\text{mv}}{\text{in}} \times 0.050 \frac{\text{in}}{\text{ma}} = 25 \frac{\text{mv}}{\text{ma}} \quad (\text{From Figure 7})$$

$$\therefore \alpha = \frac{1}{4.2 \frac{\text{ma}}{\text{mg}} \times 25 \frac{\text{mv}}{\text{ma}}} = .0095 \frac{\text{mg}}{\text{mv}} = \frac{\text{mg}}{\text{volt}}$$

Table 5. Calculation of Integrator Constant

$$\text{Work} = W = \int_{x_1}^{x_2} \vec{F} \, dx = kQ$$

$$k_X = Q,$$

But x is traversed in time t , and we can substitute:

$$W = \int_{t_1}^{t_2} F \, dt = kQ, \text{ and}$$

$$FT = kQ$$

$$\therefore k = \frac{\text{volt sec}}{\text{integrator volts}}$$

10 integrator volts read in 17.2 sec for 1 volt is:

$$k = \frac{1 \text{ volt} \times 17.2 \text{ sec}}{10 \text{ integrator volts}}$$

$$k = 1.72 \text{ sec}$$

Table 6. Coefficients of Friction for Fiber Pairs
of 7 Denier Type 280* Nylon 66

Test Number	20 mg		10 mg	
	μ_s	μ_k	μ_s	μ_k
1	.378	.244	.477	.276
2	.414	.264	.460	.268
3	.499	.326	.503	.325
4	.332	.211	.406	.230
5	.440	.240	.394	.238
6	.420	.254	.535	.275
7	.419	.268	.591	.368
8	.439	.301	.656	.373
9	.587	.286	.627	.383
10	.344	.201	.359	.176
11	.406	.229	.333	.196
12	.360	.225	.408	.208
13	.328	.211	.392	.194
14	.382	.211	.349	.172
15	.358	.184	.330	.157
16	.397	.265	.416	.245
17	.473	.265	.487	.280
18	.461	.276	.550	.297
19	.449	.276	.466	.288
20	.471	.309	.586	.305
21	.472	.269	.488	.246
22	.409	.287	.484	.291

Table 6 (Concluded). Coefficients of Friction for Fiber Pairs
of 7 Denier Type 280* Nylon 66

Test Number	20 mg		10 mg	
	μ_s	μ_k	μ_s	μ_k
23	.426	.269	.482	.287
24	.462	.338	.478	.326
25	.495	.284	.556	.280
26	.422	.305	.405	.242
27	.427	.283	.439	.271
28	.421	.245	.448	.249
29	.558	.370	.586	.428
30	.484	.294	.462	.291
31	.404	.251	.436	.251
32	.515	.296	.570	.290
33	.469	.267	.480	.241
34	.484	.287	.692	.371
35	.536	.293	.744	.375
36	.515	.395	.636	.419
37	.493	.327	.656	.389
38	.461	.333	.658	.379
39	.437	.289	.658	.412
40	.511	.284	.566	.292
41	.541	.340	.654	.320
42	.599	.351	.568	.365
43	.488	.310	.598	.343
44	.569	.323	.618	.335
45	.540	.291	.545	.313
Average	.456	.281	.517	.295
μ_s/μ_k		1.62		1.75

*

Table 7. Coefficients of Friction for Fiber Pairs
of 10 Denier Type 280* Nylon 66

Test Number	20 mg		10 mg	
	μ_s	μ_k	μ_s	μ_k
1	.396	.284	.570	.369
2	.392	.283	.534	.368
3	.475	.316	.494	.330
4	.444	.319	.560	.343
5	.509	.290	.583	.385
6	.489	.350	.545	.345
7	.375	.233	.482	.251
8	.464	.291	.482	.288
9	.487	.280	.428	.289
10	.473	.259	.561	.299
11	.389	.280	.582	.309
12	.479	.298	.685	.359
13	.418	.266	.459	.273
14	.440	.276	.473	.309
15	.535	.325	.624	.361
16	.465	.277	.451	.279
17	.449	.301	.474	.271
18	.417	.243	.416	.233
19	.470	.295	.545	.327
20	.504	.304	.711	.372
21	.541	.367	.718	.430
22	.483	.312	.590	.359

Table 7 (Concluded). Coefficients of Friction for Fiber Pairs
of 10 Denier Type 280* Nylon 66

Test Number	20 mg		10 mg	
	μ_s	μ_k	μ_s	μ_k
23	.462	.321	.604	.369
24	.467	.311	.561	.340
25	.469	.272	.680	.341
26	.590	.352	.589	.365
27	.470	.331	.537	.334
28	.543	.334	.554	.351
29	.583	.369	.699	.430
30	.510	.322	.620	.349
31	.407	.196	.930	.398
32	.437	.252	.669	.438
33	.405	.258	.786	.482
34	.432	.248	.535	.288
35	.555	.342	.714	.430
36	.511	.335	.633	.353
37	.358	.197	.422	.212
38	.404	.248	.513	.304
39	.417	.258	.485	.284
40	.446	.258	.524	.309
41	.475	.300	.514	.352
42	.451	.334	.516	.349
43	.617	.381	.696	.402
44	.701	.420	.704	.412
45	.525	.341	.672	.423
Average	.474	.299	.579	.343
μ_s/μ_k	1.58		1.69	

*

Table 8. Coefficients of Friction for Fiber Pairs
of 15 Denier Type 280* Nylon 66

Test Number	20 mg		10 mg	
	μ_s	μ_k	μ_s	μ_k
1	.462	.330	.501	.322
2	.459	.337	.574	.393
3	.501	.340	.564	.368
4	.367	.173	.487	.226
5	.507	.256	.431	.236
6	.406	.222	.484	.262
7	.597	.324	.643	.421
8	.424	.220	.523	.273
9	.458	.295	.517	.312
10	.383	.213	.513	.278
11	.422	.279	.479	.298
12	.530	.316	.552	.356
13	.519	.352	.472	.307
14	.515	.306	.588	.383
15	.520	.368	.610	.366
16	.494	.258	.496	.301
17	.517	.310	.534	.302
18	.585	.362	.645	.362
19	.431	.295	.526	.332
20	.533	.323	.601	.329
21	.528	.351	.602	.365
22	.469	.218	.585	.249
23	.443	.254	.427	.240
24	.465	.257	.604	.293
25	.412	.273	.503	.322

Table 8 (Concluded). Coefficients of Friction for Fiber Pairs
of 15 Denier Type 280* Nylon 66

Test Number	20 mg		10 mg	
	μ_s	μ_k	μ_s	μ_k
26	.538	.362	.697	.398
27	.600	.379	.710	.470
28	.467	.310	.694	.366
29	.476	.302	.547	.331
30	.471	.289	.606	.309
31	.516	.358	.768	.419
32	.460	.368	.613	.388
33	.414	.255	.517	.294
34	.515	.341	.668	.390
35	.675	.428	.672	.432
36	.698	.520	.766	.540
37	.492	.312	.653	.392
38	.711	.469	.766	.470
39	.794	.471	.820	.529
40	.589	.334	.687	.355
41	.735	.435	.905	.491
42	.719	.414	.785	.432
43	.509	.266	.660	.333
44	.641	.377	.746	.431
45	.607	.347	.753	.391
Average	.524	.326	.611	.357
μ_s/μ_k	1.61		1.71	

* Semidull Fiber

Table 9. Coefficients of Friction for Fiber Pairs
of 20 Denier Type 280* Nylon 66

Test Number	20 mg		10 mg	
	μ_s	μ_k	μ_s	μ_k
1	.534	.410	.629	.410
2	.560	.430	.702	.381
3	.573	.414	.693	.462
4	.512	.378	.640	.419
5	.591	.416	.690	.424
6	.560	.389	.640	.416
7	.507	.331	.570	.355
8	.505	.354	.593	.384
9	.435	.313	.549	.342
10	.656	.402	.695	.476
11	.556	.411	.670	.450
12	.556	.416	.668	.446
13	.577	.390	.650	.426
14	.432	.363	.619	.423
15	.535	.383	.576	.404
16	.519	.351	.565	.390
17	.659	.420	.691	.455
18	.531	.362	.715	.394
19	.485	.316	.579	.312
20	.522	.312	.801	.366
21	.411	.276	.602	.335
22	.432	.282	.572	.337
23	.547	.412	.593	.381
24	.591	.391	.696	.425

Table 9 (Concluded). Coefficients of Friction for Fiber Pairs
of 20 Denier Type 280* Nylon 66

Test Number	20 mg		10 mg	
	μ_s	μ_k	μ_s	μ_k
25	.556	.381	.631	.380
26	.609	.359	.690	.348
27	.522	.348	.600	.343
28	.435	.330	.609	.397
29	.501	.342	.557	.368
30	.451	.298	.537	.332
31	.566	.331	.724	.362
32	.414	.234	.505	.253
33	.560	.352	.654	.352
34	.555	.360	.661	.381
35	.655	.393	.725	.402
36	.578	.383	.580	.398
37	.729	.428	.855	.492
38	.696	.423	.737	.434
39	.564	.402	.655	.403
40	.536	.387	.664	.427
41	.545	.430	.595	.443
42	.637	.371	.821	.498
43	.643	.414	.826	.470
44	.663	.410	.707	.420
45	<u>.585</u>	<u>.345</u>	<u>.651</u>	<u>.389</u>
Average	.551	.370	.652	.398
1.49		1.64		

* Semidull Fiber

Table 10. Coefficients of Friction for Fiber Pairs
of 15 Denier Type 90* Nylon 66

Test Number	20 mg		10 mg	
	μ_s	μ_k	μ_s	μ_k
1	.692	.422	.740	.432
2	.594	.414	.820	.481
3	.494	.311	.641	.449
4	.530	.364	.754	.389
5	.467	.275	.611	.396
6	.474	.336	.610	.319
7	.533	.360	.658	.391
8	.618	.374	.618	.385
9	.749	.497	.746	.353
10	.541	.346	.597	.353
11	.460	.299	.567	.360
12	.565	.345	.506	.348
13	.645	.387	.552	.383
14	.575	.355	.587	.383
15	<u>.501</u>	<u>.253</u>	<u>.577</u>	<u>.357</u>
Average	.562	.355	.639	.385
μ_s/μ_k	1.58		1.65	

* Bright Fiber, Trilobal

Table 11. Coefficients of Friction for Fiber Pairs
of 15 Denier Type 680* Nylon 66

Test Number	20 mg		10 mg	
	μ_s	μ_k	μ_s	μ_k
1	.541	.404	.602	.418
2	.522	.386	.626	.400
3	.594	.430	.670	.417
4	.526	.365	.602	.362
5	.524	.386	.578	.376
6	.560	.364	.600	.369
7	.500	.315	.605	.324
8	.519	.362	.523	.316
9	.486	.344	.667	.407
10	.548	.379	.607	.360
11	.650	.370	.473	.353
12	.495	.349	.553	.389
13	.529	.323	.542	.339
14	.496	.364	.572	.365
15	.536	.355	.634	.405
16	.445	.352	.635	.395
17	.535	.361	.600	.384
18	.554	.361	.494	.375
19	.548	.364	.655	.399
20	.542	.370	.666	.391
21	.465	.366	.567	.398
22	.539	.408	.630	.408
23	.467	.376	.615	.423
24	.558	.359	.565	.385
25	.569	.438	.674	.448

Table 11 (Concluded). Coefficients of Friction for Fiber Pairs
of 15 Denier Type 680* Nylon 66

Test Number	20 mg		10 mg	
	μ_s	μ_k	μ_s	μ_k
26	.581	.404	.668	.461
27	.540	.388	.634	.431
28	.576	.415	.699	.463
29	.544	.417	.634	.416
30	.550	.378	.681	.437
31	.546	.381	.660	.423
32	.539	.401	.630	.420
33	.581	.434	.617	.390
34	.523	.381	.636	.423
35	.534	.361	.636	.408
36	.554	.401	.661	.456
37	.525	.381	.655	.441
38	.574	.435	.622	.409
39	.556	.394	.625	.386
40	.566	.364	.624	.366
41	.556	.407	.588	.396
42	.598	.378	.797	.526
43	.605	.383	.688	.431
44	.593	.386	.517	.339
45	<u>.547</u>	<u>.388</u>	<u>.638</u>	<u>.454</u>
Average	.544	.381	.620	.402
μ_s/μ_k	1.43		1.54	

* Dull Fiber

Table 12. Representative Values of the Coefficients of Friction
for Textile Fibers as Reported by Various Investigators

Investigator	Fiber	Cross- Section	Normal Force (mg)	μ_s	μ_k	μ_s/μ_k
Gunther	Cotton	Ribbon	10	0.590	0.240	2.46
Bryant	Cotton	Ribbon	20	0.523	0.292	1.80
Mercer and Makinson	Cotton	Ribbon	170-180	0.570		
Gunther	Viscose	Irregular Circle	10	0.580	0.340	1.71
Bryant	Viscose	Irregular Circle	20	0.539	0.304	1.80
Howell	Viscose	Irregular Circle	57	0.460		
Mercer and Makinson	Viscose	Irregular Circle	170-180		0.190*	
Gralen and Olafsson	Viscose	Irregular Circle	17	0.302	0.180	1.68
Gralen and Olafsson	Viscose	Irregular Circle	47	0.282	0.156	1.80
Gralen and Olafsson	Viscose	Irregular Circle	67	0.276	0.144	1.92
Gunther	Nylon 6	Circular	10	0.800	0.440	1.82
Bryant	Nylon	Circular	20	0.549	0.338	1.62
Howell	Nylon	Circular	20		0.310*	
Howell	Nylon	Circular	4		0.600*	
Mercer and Makinson	Nylon	Circular	170-180		0.230*	
Scheier and Lyons	Nylon	Circular	10	0.700		

Table 12 (Concluded). Representative Values of the Coefficients of Friction for Textile Fibers as Reported by Various Investigators

Investigator	Fiber	Cross- Section	Normal Force (mg)	μ_s	μ_k	μ_s/μ_k
Pascoe and Tabor	Nylon	Circular	10		0.500*	
Huff	Nylon 6	Trilobal	10	0.520	0.340	1.53
Huff	Nylon 6	Duokelion	10	0.530	0.350	1.52
Huff	Nylon 6	Tetrakelion	10	0.500	0.300	1.67
Huff	Nylon 6	Quasi- Triangular	10	0.520	0.290	1.79
Huff	Nylon 6	Circular	10	0.710	0.400	1.78
Huff	Nylon 6	Trilobal	2	0.820	0.540	1.54
Huff	Nylon 6	Duokelion	2	0.500	0.300	1.67
Huff	Nylon 6	Tetrakelion	2	0.920	0.560	1.64
Huff	Nylon 6	Quasi- Triangular	2	1.170	0.670	1.75
Huff	Nylon 6	Circular	2	1.420	0.610	2.32

* Approximate

Table 13. Analysis of Variance for the Effect of Fiber Diameter upon μ_s at 10 mg Normal Force

Source of Variance	Degree of Freedom	Sum of Squares	Mean Squares
Among Different Size Fibers	4	0.06024	0.01506
Within Same Size Fibers	<u>20</u>	<u>0.09600</u>	0.00480
Total	24	0.15624	

Test of Hypothesis:

$$F_4, 20 = 0.01506/0.00480 = 3.14$$

From Statistical Tables: $F_4, 20 = 2.87$ at 95% level

$$3.14 > 2.87$$

Conclusion: The differences in the μ_s data at 10 mg normal force for different diameters of Nylon 66 fibers are significant at the 95 per cent confidence level.

Table 14. Analysis of Variance for the Effect of Fiber Diameter upon μ_k at 10 mg Normal Force

Source of Variance	Degrees of Freedom	Sum of Squares	Mean Squares
Among Different Size Fibers	4	0.04404	0.01101
Within Same Size Fibers	<u>20</u>	<u>0.03640</u>	0.00182
Total	24	0.08044	

Test of Hypothesis:

$$F_4, 20 = 0.01101/0.00182 = 6.06$$

From Statistical Tables: $F_4, 20 = 2.87$ at 95% level

$$6.06 > 2.87$$

Conclusion: The differences in the μ_k data at 10 mg normal force for different diameters of Nylon 66 fibers are significant at the 95 per cent confidence level.

Table 15. Analysis of Variance for the Effect of Fiber Diameter upon μ_s at 20 mg Normal Force

Source of Variance	Degree of Freedom	Sum of Squares	Mean Squares
Among Different Size Fibers	4	0.04780	0.01196
Within Same Size Fibers	<u>20</u>	<u>0.06220</u>	0.00311
Total	24	0.11000	

Test of Hypothesis:

$$F_4, 20 = 0.1196/0.00311 = 3.84$$

From Statistical Tables: $F_4, 20 = 2.87$ at 95% level

$$3.84 > 2.87$$

Conclusion: The differences in the μ_s data at 20 mg normal force for different diameters of Nylon 66 fibers are significant at the 95 per cent confidence level.

Table 16. Analysis of Variance for the Effect of Fiber Diameter upon μ_k at 20 mg Normal Force

Source of Variance	Degree of Freedom	Sum of Squares	Mean Squares
Among Different Size Fibers	4	0.04490	0.01022
Within Same Size Fibers	<u>20</u>	<u>0.02780</u>	0.00139
Total	24	0.07270	

Test of Hypothesis:

$$F_{4, 20} = 0.01022/0.00139 = 7.36$$

From Statistical Tables: $F_{4, 20} = 2.87$ at 95% level

$$7.36 > 2.87$$

Conclusion: The differences in the μ_k data at 20 mg normal force for different diameters of Nylon 66 fibers are significant at the 95 per cent confidence level.

BIBLIOGRAPHY

LITERATURE CITED

1. G. Amontons, "On the Resistance Originating in Machines," Histoire de l'Academie Royale des Sciences avec Memoires, de Mathematique et de Physique, 206-222 (1699).
2. F. P. Bowden and D. Tabor, The Friction and Lubrication of Solids, Part II, 214-241, Oxford University Press, Cambridge (1964).
3. H. Hertz, "Ueber die Berührung fester elastischer Körper," Journal für die reine und Angewandte Mathematik 92, 156-171 (1881).
4. B. Lincoln, "Frictional and Elastic Properties of High Polymeric Materials," British Journal of Applied Physics 3, 260-263 (1952).
5. A. S. Lodge and H. G. Howell, "Friction of an Elastic Solid," Proceedings of the Physical Society of London 67 2-B, 89-97 (1954).
6. H. G. Howell, K. W. Mieszkis, and D. Tabor, Friction in Textiles, 28-53, Butterworths Scientific Publications, London (1959).
7. T. E. McBride, "Development of an Instrument to Measure Friction of Textile Fibers," Thesis for the M.S. Degree in Textile Engineering, Georgia Institute of Technology, Atlanta, Georgia (1965).
8. J. P. Bryant, "An Investigation of the Factors Which Influence the Frictional Properties of Textile Fibers," Thesis for the M.S. Degree in Textiles, Georgia Institute of Technology, Atlanta, Georgia (1966).
9. D. H. Gunther, Jr., "An Evaluation of Fiber Friction at Low Normal Forces," Thesis for the M.S. Degree in Textile Engineering, Georgia Institute of Technology, Atlanta, Georgia (1968).
10. J. O. Huff, "Measurement of the Relationship Between Textile Fiber Shapes and Their Frictional Characteristics," Thesis for the M.S. Degree in Textiles, Georgia Institute of Technology, Atlanta, Georgia (1968).
11. H. G. Howell, "The Laws of Static Friction," Textile Research Journal 23, 589-591 (1953).
12. J. D. Huntington, "Friction of Fiber Assemblies," Research London 10, 163-164 (1957).

13. H. G. Howell and J. Mazur, "Amonton's Law and Fiber Friction," Textile Institute Journal 44, T59-T69 (1953).
14. R. B. Belser and J. L. Taylor, "Frictional Properties of Cotton Fibers," Final Report, U.S.D.A. (SURDD) Grant No. 12-14-100-7661 (72), Georgia Institute of Technology, February 1, 1968.
15. M. W. Pascoe and D. Tabor, "The Friction and Deformation of Polymers," Royal Society of London Proceedings 235, 210-224 (1956).
16. M. W. Pascoe and D. Tabor, "Friction of Nylon as a Function of Load and Surface Curvature," Research London 8, S15-S17 (1955).
17. R. W. Moncrieff, Man-Made Fibers, 609-610, Chaucer Press, London (1963).
18. W. J. Lyons, "Studies of the Surface Geometry of Fibers, Part I: Preliminary Experiments," Textile Research Journal 30, 955-965 (1960).
19. S. C. Scheier and W. J. Lyons, "Studies of the Surface Geometry of Fibers, Part II: Improved Instrumentation and Representative Results on Camel Hair and Dacron," Textile Research Journal 34, 410-416 (1964).
20. S. C. Scheier and W. J. Lyons, "Measurement of the Surface Friction by an Electro-Mechanical Method," Textile Research Journal 35, 385-394 (1965).
21. F. L. Scardino and W. J. Lyons, "Fiber Surface Properties in Relation to Linear Assemblies During Processing, Part I: General Considerations; Results on the Worsted System," Textile Research Journal 37, 874-880 (1967).
22. F. L. Scardino and W. J. Lyons, "Fiber Surface Properties in Relation to Linear Assemblies During Processing, Part II: Results on the Cotton and Woolen Systems; Other Studies," Textile Research Journal 37, 982-988 (1967).
23. F. L. Scardino and W. J. Lyons, "Fiber Surface Properties in Relation to Linear Assemblies During Processing, Part III: Effects of Processing on Surface and Geometric Properties of Fibers," Textile Research Journal 37, 1005-1008 (1967).
24. B. R. Livesay, L. K. Jordan, and E. J. Scheibner, "Magnetic Behavior of Thin Films of Nickel and Gadolinium Near the Curie Point," Journal of Applied Physics 37, 1266-1267 (1966).

OTHER REFERENCES

1. Gralen, N., B. Olofsson, and J. Lindberg, "Measurement of Friction Between Single Fibers, Part VII: Physico-Chemical Views of Inter-Fiber Friction," Textile Research Journal 23, 623-628 (1953).
2. Makinson, K. R., J. Lindberg, and N. Gralen, "Measurement of Friction Between Single Fibers," Textile Research Journal 19, 97-100 (1949).
3. Mercer, E. H., "Fibers-Measuring Frictional Properties," Australian Journal of Science 7, 173-174 (1945).
4. Wine, R. L., Statistics for Scientists and Engineers, 292-361, Prentice-Hall, Inc., Englewood Cliffs, New Jersey (1964).